LBNL-6870E

USER'S MANUAL FOR THE RealGasBrine v1.0 OPTION OF TOUGH+ v1.5: A CODE FOR THE SIMULATION OF SYSTEM BEHAVIOR IN GAS-BEARING GEOLOGIC MEDIA

G.J. Moridis and C.M. Freeman

Earth Sciences Division,
Lawrence Berkeley National Laboratory,
Berkeley, CA 94720

August 2014

This work was supported by the U.S. Environmental Protection Agency through Interagency Agreement (DW-89-92235901-C) to the Lawrence Berkeley National Laboratory (a U.S. Department of Energy National Laboratory managed by the University of California under Contract No. DE-AC02-05CH11231), and by the Research Partnership to Secure Energy for America (RPSEA - Contract No. 08122-45) through the Ultra-Deepwater and Unconventional Natural Gas and Other Petroleum Resources Research and Development Program as authorized by the US Energy Policy Act (EPAct) of 2005.

PAGE LEFT INTENTIONALLY BLANK

User's Manual for the REALGASBRINE V1.0 Option of TOUGH+ v1.5: A Code for the Simulation of System Behavior in Gas-Bearing Geologic Media

G.J. Moridis and C.M. Freeman
Earth Sciences Division, Lawrence Berkeley National Laboratory
University of California, Berkeley, California

Abstract

REALGASBRINE v1.0 is a numerical code that for the simulation of the behavior of gas-bearing porous and/fractured geologic media. It is an option of TOUGH+ v1.5 [*Moridis*, 2014], a successor to the TOUGH2 [*Pruess et al.*, 1999; 2012] family of codes for multi-component, multiphase fluid and heat flow developed at the Lawrence Berkeley National Laboratory. REALGASBRINE v1.0 needs the TOUGH+ v1.5 core code in order to compile and execute. It is written in standard FORTRAN 95/2003, and can be run on any computational platform (workstation, PC, Macintosh) for which such compilers are available.

REALGASBRINE v1.0 describes the non-isothermal two- (for pure water) or three-phase (for brine) flow of an aqueous phase and a real gas mixture in a gas-bearing medium, with a particular focus in ultra-tight (such as tight-sand and shale gas) systems. Up to 12 individual real gases can be tracked, and salt can precipitate as solid halite. The capabilities of the code include coupled flow and thermal effects, real gas behavior, Darcy and non-Darcy flow, several isotherm options of gas sorption onto the grains of the porous media, complex fracture descriptions, gas solubility into water, and geomechanical effects on flow properties. REALGASBRINE v1.0 allows the study of flow and transport of fluids and heat over a wide range of time frames and spatial scales not only in gas reservoirs, but also in any problem involving the flow of gases in geologic media, including the geologic storage of greenhouse gas mixtures, the behavior of geothermal reservoirs with multi-component condensable (H_2O and CO_2) and non-condensable gas mixtures, the transport of water and released H_2 in nuclear waste storage applications, etc.

PAGE LEFT INTENTIONALLY BLANK

TABLE OF CONTENTS

LIST OF FIGURES

LIST OF TABLES

PAGE LEFT INTENTIONALLY BLANK

1.0. Introduction

1.1. Background

To a large part, the impetus for the development of the REALGASBRINE v1.0 application option was provided by the importance of ultra-tight natural gas reservoirs (such as shale gas reservoirs), production from which has virtually exploded over the last decade because of the advent of effective reservoir stimulation technologies. While the code has wide application to any problem involving the storage and flow of gases in geologic media, the linkage to tight gas reservoirs is obvious, as attested to by as some of the code features and capabilities (e.g., gas sorption and non-Darcy flows) that were introduced to address the particular needs of such reservoirs. Thus, the introduction cannot but address this subject.

The ever-increasing energy demand, coupled with the advent and advances in reservoir stimulation technologies, has prompted an explosive growth in the development of unconventional gas resources in the U.S. during the last decade. Tight-sand and shale gas reservoirs are currently the main unconventional resources, upon which the bulk of production activity is currently concentrating [*Warlick*, 2006]. Production from such resources in the U.S. has skyrocketed from virtually nil at the beginning of 2000, to 6% of the gas produced in 2005 [*U.S. EIA*, 2007], to 23% in 2010, and is expected to reach 49% by 2035 [*U.S. EIA*, 2012]. Production of shale gas is expected to increase from a 2007 U.S. total of 1.4 TCF to 4.8 TCF in 2020 [*API*, 2013]. In its Annual Energy Outlook for 2011, the US Energy Information Administration (EIA) more than doubled its estimate of technically recoverable shale gas reserves in the US from 353 TCF to 827 TCF by including data from recent drilling results in the Marcellus, Haynesville, and Eagle Ford shales [*US EIA*, 2011]. Note that the bulk of the gas production from tight sands and shales has concentrated almost exclusively in North America (U.S. and Canada), and serious production elsewhere in the rest world has yet to begin. This leads to reasonable expectations that gas production from such ultra-tight systems may be one of the main sources (if not the main) source of natural gas in the world for decades to come, with obvious economic and geostrategic implications, and significant benefits for national economies and national energy security.

The importance of tight-sand and shale reservoirs as energy resources necessitates the ability to accurately estimate reserves and to evaluate, design, manage and predict production from such systems over a wide range of time frames and spatial scales. Modeling and simulation play a key role in providing the necessary tools for these activities. However, these reservoirs present challenges that cannot easily (if at all) handled by conventional gas models and simulators: they are characterized by extremely low permeabilities (often in the nD = 10^{-21} m^2 range), have native fractures that interact with the fractures created during the reservoir stimulation and with the matrix to result in very complicated flow regimes that very often deviate from Darcy's Law, have pores very small pores that interfere with the Brownian motion of the gas molecules (thus rendering predictions from standard advection-based models dubious, if not irrelevant, as they requiring accounting for Knudsen and multi-component diffusion), exhibit highly non-linear behavior, have large amounts of gas sorbed onto the grains of the porous media in addition to gas stored in the pores, and may exhibit unpredictable geomechanical behavior such as the evolution of secondary fractures [*Kim and Moridis*, 2013] that may further complicate an already complex flow regime.

Several analytical and semi-analytical models have been proposed to predict flow performance and production from these ultra-tight reservoirs [*Gringarten*, 1971; *Gringarten et al*., 1974, *Blasingame and Poe*, 1993; *Medeiros et al*., 2006; *Bello and Wattenbarger*, 2008; *Mattar*, 2008; *Anderson et al*., 2010]. Most of these studies have assumed idealized and regular fracture geometries, include significant simplifying assumptions and cannot accurately handle the very highly nonlinear aspects of shale-gas and tight-gas reservoirs, cannot describe complex domain geometries, and cannot accurately capture gas sorption and desorption from the matrix (a non-linear process that does not lend itself to analytical solutions), multiphase flow, consolidation, and several non-ideal and complex fracture networks [*Houze et al*., 2010]. Thus, their role as decision-making tools is limited, making numerical simulators the only practical option.

The economic importance of the energy resources in such ultra-tight reservoirs and the shortcomings of the analytical and semi-analytical models have led to the development of numerical reservoir simulators that address the particularities of these systems. *Miller et al.* [2010] and *Jayakumar et al*. [2011] used numerical simulation to history-match and forecast production from two different shale-gas fields. *Cipolla et al*. [2009], *Freeman* [2010], *Moridis et al.* [2010] and *Freeman et al*. [2011; 2013] and conducted numerical sensitivity studies to identify the most important mechanisms and factors that affect shale-gas reservoir performance.

Powerful commercial simulators with specialized options for shale gas analysis such as GEM [*CMG*, 2013] and ECLIPSE For Unconventionals [*SLB*, 2013] have become available. While these address the most common features of unconventional and ultra-tight media, they are designed primarily for large-scale production evaluation at the reservoir level and cannot be easily used for scientific investigations of micro-scale processes and phenomena in the vicinity of fractures.

The TOUGH+ v1.5 code with the REALGASBRINE v1.0 application (hereafter collectively referred to as **T+RGB**) described in this report is capable of simulating processes and phenomena of flow through a wide variety of geological media (from very permeable to ultra-tight, porous and fractured) over a range of scales that varies from the mm- to the field-level. This report describes underlying physics and thermodynamics of **T+RGB**, lists and explains the data inputs required for its application, and discusses several applications to problems of flow and transport in gas-bearing media.

1.2. The TOUGH+ Family of Codes

TOUGH+ v1.5 is a family of public domain codes developed at the Lawrence Berkeley National Laboratory [*Moridis*, 2014] as a successor to the TOUGH2 [*Pruess et al*., 1999; 2012] family of codes for multi-component, multiphase fluid and heat flow. It employs dynamic memory allocation, follows the tenets of Object-Oriented Programming (OOP), and involves entirely new data structures and derived data types that describe the objects upon which the code is based. It is written in standard FORTRAN 95/2003, and can be run on any computational platform (workstations, PC, Macintosh).

By using the capabilities of the FORTRAN95/2003 language, the new OOP architecture involves the use of pointers, lists and trees, data encapsulation, defined operators and assignments, operator extension and overloading, use of generic procedures, and maximum use of the powerful intrinsic vector and matrix processing operations (available in the extended mathematical library of FORTRAN 95/2003). This leads to increased computational efficiency, while allowing seamless applicability of the code to multi-processor parallel computing platforms. The result is a code that is transparent and compact, and frees the developer from the tedium of tracking the disparate attributes that define the objects, thus enabling a quantum jump in the complexity of problem that can be tackled. An additional feature of the FORTRAN 95/2003 language of TOUGH+ is the near complete interoperability with C/C++, which allows the interchangeable use of procedures written in either FORTRAN 95/2003 or C/C++, makes possible the seamless coupling with external packages (such as the geomechanical commercial code FLAC3D [*Itasca*, 2002]) and interaction with pre- and post-processing graphical environments.

TOUGH+ v1.5 has a completely modular architecture. Any member of the TOUGH+ family of codes comprises three components: (a) the core TOUGH+ code that is common to all applications related to the study of non-isothermal processes of flow and transport through geologic media, (b) the code that is *unique* to a particular type of application/problem (e.g., the properties and flow of a crude oil, the flow of water and air through geologic media, etc.), and (c) supplemental TOUGH+ code units that describe special physics and processes that are encountered in particular types of problems (e.g., code units that describe real gas properties, non-Darcian flow processes, salinity effects on the properties of water, etc.) and are *used by more than one* application options.

Thus, the core TOUGH+ code – which is distributed as a separate entity by LBNL– cannot conduct any simulations by itself, but needs additional units of supplemental and problem-specific code before it can become operational. The additional code solves the equation of state (EOS) corresponding to the specific problem; it is called an ***application option*** or simply an ***option*** in the TOUGH+ nomenclature and is distributed as a separate entity/product by LBNL. The term ***option*** – rather the older term ***module*** or ***EOS*** that were used in the TOUGH2 [*Pruess et al.*, 1999] nomenclature – is used to avoid confusion, as the word *module* has a particular meaning in the FORTRAN 95/2003 language of TOUGH+.

1.3. The REALGASBRINE v1.0 Code

REALGASBRINE v1.0 is the TOUGH+ v1.5 application option that describes the non-isothermal two- (for pure water) or three-phase (for brine) flow of an aqueous phase and a real gas mixture in any type of gas bearing medium, with a particular focus in ultra-tight (such as tight-sand and shale gas) systems. The gas mixture is treated as either a single-pseudo-component having a fixed composition, or as a multicomponent system composed of up to 12 individual real gases, including CO_2. In the case of brine, the salt can precipitate as solid halite under appropriate conditions, leading to reductions in porosity and permeability.

In addition to the standard capabilities of all members of the TOUGH+ family of codes (fully-implicit, compositional simulators using both structured and unstructured grids), the capabilities of the code include: coupled flow and thermal effects in porous and/or fractured media, real gas behavior, gas slippage (Klinkenberg) effects, full micro-flow treatment (Knudsen diffusion [*Freeman et al.*, 2011] and Dusty Gas Model [*Webb*, 1998]), Darcy and non-Darcy flow through the matrix and fractures of fractured media, single- and multi-component gas sorption onto the grains of the porous media following several isotherm options, discrete and equivalent fracture representation, porosity-permeability dependence on pressure changes, complex matrix-fracture relationships with generalized fracture effect concepts such as dual- and multi-porosity [*Warren and Root*, 1963], dual-permeability, and multiple interactive continua [*Pruess*, 1983; *Doughty*, 1999], etc.. The code involves robust physics of gas dissolution into water/brine, and the most updated thermodynamics describing the behavior of gaseous components and water.

The **T+RGB** v1.0 code account for practically all known processes and phenomena, involve a minimum of assumptions, and are suitable for scientific investigations at any spatial (from the sub-mm scale in the vicinity of the fracture surface to the reservoir scale) and temporal scales, thus allowing insights into the system performance and behavior during production. It can provide solutions to the problem of prediction of gas production from the entire spectrum of gas-bearing reservoirs, but also of any reservoir involving water and gas mixtures of up to 12 components (including H_2O vapor). The code can simulate problems of any scale, ranging from mm-scale processes at the imbibing surface of a hydraulic fracture to core-scale studies to field-scale investigations. The only limitations on the size of the domain to be simulated are imposed by the underlying physics and by the capabilities of the computational platform. Thus, if the volume of the domain and its subdivision are such that (a) a representative volume can be defined and (b) the flow of fluids can be adequately described by a macro-scale model, then **T+RGB** can predict the system behavior.

Note that, although the main impetus for the development of **T+RGB** was the need to analyze and understand the problems of flow of water/brine and hydrocarbon gases through tight reservoirs, it is important to indicate that the code is fully applicable to a wide variety of other problems, including the study of the geologic storage of greenhouse gas mixtures, the behavior of geothermal reservoirs with multi-component condensable (H_2O and CO_2) and non-condensable gas mixtures, the transport of water and released H_2 in nuclear waste storage applications, etc..

This report provides a detailed presentation of the features and capabilities of **T+RGB**, and includes a thorough discussion of the underlying physical, thermodynamic and mathematical principles of the model in addition to the main governing equations. The various phase regimes and the corresponding primary variables are discussed in detail, as well as the reasons for their selection. Examples of input data files, of the corresponding output files, as well as the results from these illustrative sample problems of gas production from realistic gas-bearing geologic systems, are included as an aide to the **T+RGB** user.

2.0 Concepts, Underlying Physics, and Governing Equations

2.1. Modeled Processes and Underlying Assumptions

T+RGB can model the following processes and phenomena in gas-bearing geologic systems:

(1) The flow of gases and liquids in the porous/fractured geologic system by Darcian and/or non-Darcian physics

(2) The corresponding heat flow and transport

(3) The partitioning of the mass components among the possible phases

(4) Heat exchanges due to

   a. Conduction

   b. Advection/convection

   c. Radiation

   e. Latent heat related to phase changes (ice melting or water fusion, water evaporation or vapor condensation)

   f. Gas dissolution
   g. Salt dissolution

(5) Gas sorption onto the grains of the porous media

(6) The transport of salt in the aqueous phase, accounting for advection and molecular diffusion

(7) The precipitation salt as halite if its concentration in the aqueous phase exceeds its solubility

(8) The effects of salt on the thermophysical properties of water (density, viscosity, vapor pressure, enthalpy, etc.)

A deliberate effort was made to keep the simplifying assumptions involved in the development of the underlying physical, thermodynamic and mathematical model to a minimum. These include:

(1) Flow in the domain can be described by one or more of the Darcian and non-Darcian models available in **T+RGB**.

(2) In the transport of dissolved gases and salts, mechanical dispersion is small compared to advection (by neglecting mechanical dispersion, memory requirements and execution times are substantially reduced).

(3) The pressure P < 100 MPa (14,504 psi). The pressure-dependent equations describing the water properties and behavior in **T+RGB** provide accurate solutions for practically the entire spectrum of conditions encountered in natural geologic media. Thus, the existing capabilities can easily accommodate any natural or laboratory system. Although equations for an accurate description of the thermophysical properties of gas+H2O systems for P as high as 1000 MPa are

available in the code, this option is disabled because it involves an iterative process that increases the execution time by a factor of 3 or 4 even for $P < 100$ MPa.

2.2. Components and Phases

A non-isothermal gas + H_2O system can be fully described by the appropriate mass balance equations and an energy balance equation. The following components κ (and the corresponding indicators used in the subsequent equations), corresponding to the number of equations, are considered in **T+RGB**:

$\kappa \equiv$	g^i	the various gaseous components i ($i = 1, \ldots, N_G$, $N_G \geq 1$) constituting the gas mixture.
	w	water
	s	salt
	θ	heat

The following 12 gases are available in T+RGB: CH_4, C_2H_6, C_3H_8, n-C_4H_{10}, i-C_4H_{10}, H_2O, CO_2, H_2S, O_2, N_2 C_2H_5OH, and H_2, of which only H_2O, CO_2 and C_2H_5OH are condensable. These are included as standard entries into the database of the TOUGH+ v1.5 supplemental code unit **`T_RealGas_Properties.f95`** [*Moridis*, 2014].

In **T+RGB**, if the circumstances warrant it, it is possible to treat the H_2O-free part of a real gas mixture as a *single pseudo-component* (i.e., $N_G = 1$) of constant composition (i.e., with non-variant mole fractions Y^i of the individual gases), the properties of which vary with the pressure P and temperature T. In that case, the gas phase comprises two components: the H_2O and the H_2O-free pseudo-component. The composition of the gas phase may still change (because of the near-universal presence of H_2O vapor in the subsurface), but the composition of the individual gases that constitute the pseudo-component is treated as invariant. Air is a good example of such a pseudo-component for **T+RGB** applications.

Note that heat is included in this list as a pseudo-component (as the heat balance is tracked similarly to the mass balance of the individual mass components) for the purpose of defining the maximum number of simultaneous equations to be solved. Thus, the list indicates that the maximum number of mass components that may be considered in a problem involving pure water and a gas mixture of N_G constituents is N_G+1; for a brine, the number of mass components is N_G+2. The corresponding maximum number of simultaneous equations that need to be solved is (a) $N_E = N_G +1$ and $N_E = N_G +1$ (for isothermal and non-isothermal conditions, respectively) when no salt is present, and (b) and $N_E = N_G +2$ and $N_G +3$ (for isothermal and non-isothermal conditions, respectively) when salt is present.

These mass and energy components are partitioned among two or three possible phases β (corresponding to the absence and presence of salt, respectively) which are listed below along with the corresponding indicators (used in the subsequent equations):

$\beta \equiv$	A	aqueous (components: liquid w, dissolved s, N_G dissolved gases)
	G	gaseous (components: N_G gases, vapor w)
	H	solid: precipitated halite (components: s; phase included ONLY when salt is considered)

2.3. The Mass and Energy Balance Equation

Following *Pruess et al.* [1999; 2012], mass and heat balance considerations in every subdomain (gridblock) into which the simulation domain is been subdivided by the integral finite difference method dictates that

$$\frac{d}{dt}\int_{V_n} M^{\kappa}\, dV = \int_{\Gamma_n} \mathbf{F}^{\kappa} \cdot \mathbf{n}\, d\tilde{A} + \int_{V_n} q^{\kappa}\, dV \,, \tag{2.3}$$

where:

V, V_n	volume, volume of subdomain n [L^3];
M^{κ}	mass accumulation term of component κ [kg m^{-3}];
A, Γ_n	surface area, surface area of subdomain n [L^2];
$\mathbf{F}^{\kappa}$	Darcy flux vector of component κ [kg m^{-2}s^{-1}];
$\mathbf{n}$	inward unit normal vector;
q^{κ}	source/sink term of component κ [kg m^{-3}s^{-1}];
t	time [T].

2.4. Mass Accumulation Terms

Under equilibrium conditions, the mass accumulation terms M^{κ} for the mass components in equation (2.3) are given by

$$M^{\kappa} = \sum_{\beta \equiv A,G,H} \phi S_{\beta} \rho_{\beta} X_{\beta}^{\kappa} + \delta_{\Psi}^{i} (1-\phi) \rho_R \Psi^{i} \,, \quad \kappa \equiv w, g^{i}, s, \quad i = 1,\ldots,N_G \tag{2.4}$$

where

ϕ	porosity [*dimensionless*];

ρ_β	density of phase β [kg m^{-3}];
S_β	saturation of phase β [*dimensionless*];
X_β^κ	mass fraction of component $\kappa \equiv w,m,i$ in phase β [kg/kg]
Ψ^i	the mass of sorbed component g^i per unit mass of rock [kg/kg]
δ_Ψ^i	= 0 for non-sorbing species on a given medium (including tight-gas systems) that are usually devoid of substantial organic carbon; δ_Ψ^i = 1 in gas-sorbing species onto a given medium. Obviously, $\delta_\Psi^s = 0$.

The first term in Equation (2.4) describes fluid mass stored in the pores, and the second the mass of gaseous components sorbed onto the organic carbon (mainly kerogen) content of the matrix of the porous medium. The latter is quite common in shales. Although gas desorption from kerogen has been studied extensively in coalbed CH_4 reservoirs, and several analytic/semi-analytic models have been developed for such reservoirs [*Clarkson and Bustin*, 1999], the sorptive properties of shale are not necessarily analogous to coal [*Schettler and Parmely*, 1991].

The most commonly used empirical model describing sorption onto organic carbon in shales is analogous to that used in coalbed methane and follows the Langmuir isotherm that, for a single-component gas, is described by

$$\begin{cases} \Psi^i = \dfrac{p_{dG} m_L}{p_{dG} + p_L} & \text{for ELaS} \\ \dfrac{d\Psi^i}{dt} = k_L \left(\dfrac{p_{dG} m_L}{p_{dG} + p_L} - \Psi^i \right) & \text{for KLaS} \end{cases}, \tag{2.5}$$

where p_{dG} is the dry gas pressure ($p_{dG} = p_G - p^v$, where p^v is the partial pressure of the water vapor), ELaS indicates Equilibrium Langmuir Sorption, and KLaS denotes Kinetic Langmuir Sorption. The m_L term in Equation (2.5) describes the total mass storage of component g^i at infinite pressure (kg of gas/kg of matrix material), p_L is the pressure at which half of this mass is stored (Pa), and k_L is a kinetic constant of the Langmuir sorption (1/s). In most studies, an *instantaneous equilibrium* is assumed to exist between the sorbed and the free gas, i.e., there is no transient lag between pressure changes and the corresponding sorption/desorption responses and the equilibrium model of Langmuir sorption is assumed to be valid. Although this appears to be a good approximation in shales [*Gao et al*., 1994] because of the very low permeability of the matrix (onto which the various gas components are sorbed), the subject has not been fully investigated.

For multi-component gas, equation (3) becomes

$$\begin{cases} \Psi^i = \dfrac{p_{dG} B^i m_L^i \Upsilon^i}{1 + p_{dG} \sum\limits_i B^i \, \Upsilon^i} & \text{for ELaS} \\ \dfrac{d\Psi^i}{dt} = k_L^i \left(\dfrac{p_{dG} B^i m_L^i \Upsilon^i}{1 + p_{dG} \sum\limits_i B^i \, \Upsilon^i} - \Psi^i \right) & \text{for KLaS} \end{cases}, \tag{2.6}$$

where B^i is the Langmuir constant of component g^i in 1/Pa [*Pan and Connell*, 2009], and Y^i is the dimensionless mole fraction of the gas component *i* in the water-free gas phase. Note that the **T+RGB** code offers the additional options of linear and Freundlich sorption isotherms (equilibrium and kinetic). For each gas component g^i, these are described by the following equations:

$$\begin{cases} \Psi^i = K_l^i \, p^i & \text{for ELiS} \\ \dfrac{d\Psi^i}{dt} = k_l^i \left(K_l^i \, p^i - \Psi^i \right) & \text{for KLiS} \end{cases} \quad \text{and} \quad \begin{cases} \Psi^i = K_F^i \, \left(p^i\right)^c & \text{for EFS} \\ \dfrac{d\Psi^i}{dt} = k_F^i \left[K_F^i \, \left(p^i\right)^c - \Psi^i \right] & \text{for KFS} \end{cases} \tag{2.7}$$

where ELiS and KLiS denote Equilibrium and Kinetic Linear Sorption, respectively; EFS and KFS denote Equilibrium and Kinetic Freundlich Sorption, respectively; K^i_l and K^i_F are the distribution coefficients of the ELiS and EFS sorption isotherms of gas component *i*, respectively; p^i is the partial pressure of g^i; k^i_l and k^i_F are the kinetic coefficients of the ELiS and EFS sorption isotherms of g^i, respectively; and c is the exponent of the Freundlich sorption isotherm

2.5. Heat Accumulation Terms

The heat accumulation term includes contributions from the rock matrix and all the phases, and, in the kinetic model, is given by the equation

$$M^{\theta} = (1-\phi)\rho_R \int_{Tref}^{T} C_R(T)\, dT + \sum_{\beta=A,G,H} \phi S_\beta \rho_\beta U_\beta + \delta^i_\Psi (1-\phi)\rho_R \sum_{i=1}^{N_G} u^i \Psi^i , \qquad (2.8)$$

where

ρ_R	rock density [kg m^{-3}];
C_R	heat capacity of the dry rock [J kg^{-1} K^{-1}];
U_β	specific internal energy of phase β [J kg^{-1}];
u^i	specific internal energy of sorbed gas component g^i [J kg^{-1}];
T_{ref}	a reference temperature [k];

The specific internal energy of the gaseous phase is a very strong function of composition, is related to the specific enthalpy of the gas phase H_G, and is given by

$$U_G = \sum_{\kappa=w,g^i(i=1,N_G)} X^\kappa_G\, u^\kappa + U_{dep} \left(= H_G - \frac{P}{\rho_G} \right), \qquad (2.9)$$

where u^κ_G is the specific internal energy of component κ in the gaseous phase, and U_{dep} is the specific internal energy departure of the gas mixture [J kg^{-1}].

The internal energy of the aqueous phase accounts for the effects of gas and salt solution, and is estimated from

$$U_A = X_A^w u^w + \sum_{i=1}^{N_G} X_A^{g^i} \left(u^i + U_{sol}^i \right), \tag{2.10}$$

where u_A^w and u_A^i are the specific internal energies of the H_2O and of the natural gas component g^i at the p and T conditions of the aqueous phase, respectively, and U^i_{sol} are the specific internal energies of dissolution of the gas component g^i in H_2O (obtained from tables). Note that the reference state for all internal energy and enthalpy computations are $p = 101300$ Pa and $T = 273.15$ K (0 °C).

The salt-related term u_A^s and U_H are determined from

$$u_A^s = h_A^s - \frac{P}{\rho_i} = \int_{T_{ref}}^{T} C_s dT - \frac{P}{\rho_s} \quad \text{and} \quad U_H = H_H - \frac{P}{\rho_H} = \int_{T_{ref}}^{T} C_H dT - \frac{P}{\rho_H} \tag{2.11}$$

where T_0 is a reference temperature, h_A^s and H_H are the specific enthalpies of the salt and halite (phase), respectively, and C_i and C_H are the temperature-dependent heat capacities of the salt and the halite, respectively [J kg^{-1} K^{-1}].

2.6. Flux Terms

The mass fluxes of water, gases and salt include contributions from the aqueous and gaseous phases, i.e.,

$$\mathbf{F}^\kappa = \sum_{\beta \equiv A,G} \mathbf{F}_\beta^\kappa, \ \kappa \equiv w, g^i, \ i = 1, \ldots, N_G \tag{2.12}$$

Because it is immobile, the contribution of the solid phase ($\beta \equiv H$) to the fluid fluxes is zero. For any mobile phase β, $\mathbf{F}_\beta^\kappa = X_\beta^\kappa \mathbf{F}_\beta$.

In **T+RGB** there are three options to describe the phase flux $\mathbf{F}_\beta$. The first is the standard Darcy's law, i.e.,

$$\mathbf{F}_\beta = \rho_\beta \left[-\frac{k\, k_{r\beta}}{\mu_\beta} \nabla \Phi_\beta \right] = \rho_\beta \mathbf{v}_\beta, \;\; \nabla \Phi_\beta = \nabla p_\beta - \rho_\beta \mathbf{g}, \tag{2.13}$$

where

k	rock intrinsic permeability [m^2];
k_{rA}	relative permeability of the aqueous phase [dimensionless];
μ_A	viscosity of the aqueous phase [Pa s];
P_A	pressure of the aqueous phase [Pa];
$\mathbf{g}$	gravitational acceleration vector [m s^{-2}].

In **T+RGB**, the relationship between the aqueous and the gas pressures, p_A and p_G, respectively, is given

$$P_A = P_G + P_{cGW}\,, \;\text{ where }\; P_G = \sum_{i=1,\ldots,N_G} P_G^i + P_G^w \tag{2.14}$$

is the gas pressure [Pa], P_{cGW} is the gas-water capillary pressure [Pa], and P_G^i, P_G^w are the partial pressures [Pa] of the gas g^i and of the water vapor in the gas phase, respectively.

In **T+RGB**, the gas solubility in the aqueous phase cannot be satisfied by the simple approach of using Henry's law with a T-dependent Henry's coefficient that is standard in TOUGH+ v1.5 [*Moridis*, 2014] because this would lead to erroneous results when multi-component gases dissolve into brines. Thus, the much more involved option of determining the solubility by determining the chemical activities of the solution and by invoking the equality of in the aqueous and the gas phase.

The mass flux of the gaseous phase ($\beta \equiv G$) incorporates advection and diffusion contributions, and is given by

$$\mathbf{F}_G^\kappa = -k_0 \left(1 + \frac{b}{P_G}\right) \frac{k_{rG}\rho_G}{\mu_G} X_G^\kappa \left(\nabla P_G - \rho_G \mathbf{g}\right) + \mathbf{J}_G^\kappa, \quad \kappa \equiv w, g^i \tag{2.15}$$

where

k_0 absolute permeability at large gas pressures (= k) [m^2];

b *Klinkenberg* [1941] b-factor accounting for gas slippage effects [Pa];

k_{rG} relative permeability of the gaseous phase [*dimensionless*];

μ_G viscosity of the gaseous phase [Pa s].

Methods to estimate the b-factor are discussed in Section 4.

The term $\mathbf{J}_G^\kappa$ is the diffusive mass flux of component κ in the gas phase [kg/m^2/s], and is described by

$$\mathbf{J}_G^\kappa = -\phi S_G \underbrace{\left(\phi^{1/3} S_G^{7/3}\right)}_{\tau_G} D_G^\kappa \rho_G \nabla X_G^\kappa = -\phi\left(\tau_G\right) D_G^\kappa \rho_G \nabla X_G^\kappa, \quad \kappa \equiv w, m \tag{2.16}$$

where D_G^κ is the multicomponent molecular diffusion coefficient of component κ in the gas phase in the absence of a porous medium [m^2 s^{-1}], and τ_G is the gas tortuosity [dimensionless]. Several methods to compute τ_G are discussed by *Moridis and Pruess* [2014]. The diffusive mass fluxes of the water vapor and of the g^i (i = 1,…,N_G) gases are related through the relationship of *Bird et al.* [1960]

$$\mathbf{J}_G^w + \sum_{i=1,\dots,N_G} \mathbf{J}_G^i = 0, \tag{2.17}$$

which ensures that the total diffusive mass flux of the gas phase is zero with respect to the mass average velocity when summed over the N_G +1 components. Then the total gas phase mass flux is the product of the Darcy velocity and density of the gas phase.

The flux of the dissolved salt is described by

$$\mathbf{F}_A^s = X_A^s \mathbf{F}_A + \mathbf{J}_W^s \,, \tag{2.18}$$

where

$$\mathbf{J}_W^s = -\phi S_W \left(\phi^{1/3} S_A^{7/3} \right) \; D_A^s \rho_A \nabla X_A^s = -\phi S_W \left(\tau_A \right) \; D_A^s \rho_A \nabla X_A^s \,, \tag{2.19}$$

D_A^i is the molecular diffusion coefficient of salt in water, and τ_A is the medium tortuosity of the aqueous phase.

If the flow is non-Darcian because of inertial (turbulent) effects, then the equation $\mathbf{F}_\beta = \rho_\beta \mathbf{v}_\beta$ still applies, but $\mathbf{v}_\beta$ is now computed from the solution of the quadratic equation

$$\nabla \Phi_\beta = -\left(\frac{\mu_\beta}{k \, k_{r\beta}} \mathbf{v}_\beta + \beta_{F\beta} \rho_\beta \mathbf{v}_\beta \left| \mathbf{v}_\beta \right| \right). \tag{2.20}$$

in which β_β is the "turbulence correction factor" [*Katz et al.,* 1959]. The quadratic equation in (2.20) is the general momentum-balance *Forcheimer equation* [*Forchheimer*, 1901; *Wattenbarger and Ramey*, 1968], and incorporates inertial and turbulent effects. This is the second option. The solution then is

$$\mathbf{v}_\beta = \frac{2 \nabla \Phi_\beta}{\dfrac{\mu_\beta}{k \, k_{r\beta}} + \sqrt{\left(\dfrac{\mu_\beta}{k \, k_{r\beta}} \right)^2 + 4 \beta_{F\beta} \rho \left| \nabla \Phi_\beta \right|}} \,, \tag{2.21}$$

and the $\mathbf{v}_\beta$ from equation (2.21) is then used in the equation of flow (2.13). **T+RGB** offers 13 options to compute $\beta_{F\beta}$ several of which are listed in *Finsterle* [2001]. The third option follows the approach of *Barree and Conway* [2007], as described by *Wu et al.* [2011], which involves a different formulation of $\nabla\Phi_\beta$.

The heat flux accounts for conduction, advection and radiative heat transfer, and is given by

$$\mathbf{F}^\theta = -\bar{k}_\theta \nabla T + f_\sigma \sigma_0 \nabla T^4 + \sum_{\beta\equiv A,G} h_\beta \mathbf{F}_\beta\,, \qquad (2.22)$$

where

$\bar{k}_\theta$ composite thermal conductivity of the medium/fluid ensemble [W m^{-1} K^{-1}];

h_β specific enthalpy of phase $\beta \equiv A,G$ [J kg^{-1}];

f_σ radiance emittance factor [dimensionless];

σ_0 Stefan-Boltzmann constant [5.6687×10^{-8} J m^{-2} K^{-4}].

Several options to estimate $\bar{k}_\theta$ are discussed in *Moridis and Pruess* [2014].

The specific enthalpy of the gas phase is computed as

$$H_G = \sum_{\kappa\equiv w,g^i} X_G^\kappa h_G^\kappa + H_{dep}\,, \qquad (2.23)$$

where h_G^κ is the specific enthalpy of component κ in the gaseous phase, and H_{dep} is the specific enthalpy departure of the gas mixture [J kg^{-1}]. The specific enthalpy of the aqueous phase is estimated from

$$H_A = X_A^w h_A^w + \sum_{\kappa=1,\dots,N_{d\kappa}} X_A^\kappa \left(h_A^\kappa + H_{sol}^\kappa \right), \qquad (2.24)$$

where $N_{d\kappa}$ is the total number of *dissolved* components (including the salt, if present), h_A^κ are the specific enthalpies of various dissolved components at the conditions prevailing in the aqueous phase, respectively, and H_{sol}^{κ} is the specific enthalpy of dissolution [J kg^{-1}] of component κ in the aqueous phase, respectively.

2.7. Source and Sink Terms

In sinks with specified mass production rate, withdrawal of the mass component κ is described by

$$\hat{q}^{\kappa} = \sum_{\kappa \equiv A,G} X_{\beta}^{\kappa} q_{\beta} , \quad \kappa \equiv w, g^{i}, s, \;\; i = 1 ,..., N_G \tag{2.25}$$

where q_{β} is the production rate of the phase β [kg m^{-3}]. For a prescribed production rate, the phase flow rates q_{β} are determined internally according to the general different options available in the TOUGH+ code (see *Moridis and Pruess* [2014]). For source terms (well injection), the addition of a mass component κ occurs at desired rates $\hat{q}^{\kappa}$ ($\kappa \equiv w, g^{i}, s$). Salt injection can occur either as a rate as an individual mass component ($\hat{q}^{i}$) or as a fraction of the aqueous phase injection rate, i.e., $\hat{q}^{i} = X_{A}^{i} \hat{q}_{A}$, where X_{A}^{i} is the salt mass fraction in the injection stream.

The rate of heat removal or addition includes contributions of (a) the heat associated with fluid removal or addition, as well as (b) direct heat inputs or withdrawals q_d (e.g., microwave heating), and is described by

$$\hat{q}^{\theta} = q_d + \sum_{\beta = A,G} h_{\beta} q_{\beta} \tag{2.26}$$

2.8. Micro-Flows

2.8.1. Knudsen Diffusion

For ultra-low permeability media (e.g., tight sands and shales) and the resulting micro-flows, **T+RGB** estimates a Klinkenberg *b*-factor for a single-component or pseudo-component gas by the method of *Florence et al.* [2007] and *Freeman et al.* [2011] as

$$\frac{b}{P_G} = \left(1 + \alpha_K K_n\right)\left(1 + \frac{4K_n}{1+K_n}\right) - 1, \tag{2.27}$$

where K_n is the Knudsen diffusion number (dimensionless), which characterizes the deviation from continuum flow, accounts for the effects of the mean free path of gas molecules $\bar{\lambda}$ being on the same order as the pore dimensions of the porous media, and is computed from [*Freeman et al.*, 2011] as

$$K_n = \frac{\bar{\lambda}}{r_{pore}} = \frac{\mu_G}{2.81708 p_G}\sqrt{\frac{\pi R T}{2M}\frac{\phi}{k}}, \tag{2.28}$$

with M being the molecular weight and T the temperature (K). The term a_K in Eq. 24 is determined from Karniadakis and Beskok (2001) as

$$\alpha_K = \frac{128}{15\pi^2}\tan^{-1}\left(4K_n^{0.4}\right), \tag{2.29}$$

For simplicity, we have omitted the "*i*" superscript in Equations (27) to (29). The Knudsen diffusion can be very important in porous media with very small pores (on the order of a few micrometers or smaller) and at low pressures. For a single gas pseudo-component, the properties in (29) are obtained from an appropriate equation of state for a real-gas mixture of constant composition Y^i. The Knudsen diffusivity D_K [m^2/s] can be computed as proposed by *Civan* [2008] and *Freeman et al.* [2011].

$$D_K = \frac{4\sqrt{k\phi}}{2.81708}\sqrt{\frac{\pi RT}{2M}} \quad \text{or} \quad D_K = \frac{kb}{\mu_G} \tag{2.30}$$

2.8.2. Dusty Gas Model

For a multicomponent gas mixture that is not treated as a single pseudo-component, ordinary Fickian diffusion must be taken into account as well as Knudsen diffusion**.** Use of the advective–diffusive flow model (Fick's law) should be restricted to media with $k \geq 10^{-12}$ m^2; the dusty-gas model (DGM) is more accurate at lower k [*Webb*, 1983; *Webb and Pruess*, 2003]. Additionally, DGM accounts for molecular interactions with the pore walls in the form of Knudsen diffusion. Shales may exhibit a permeability k as low as 10^{-21} m^2, so the DGM described below is more appropriate than the Fickian model [*Webb and Pruess*, 2003; *Doronin and Larkin,* 2004; *Freeman et al*., 2011]:

$$\sum_{j=1,j\neq i}^{N_G} \frac{Y^i N_D^j - Y^j N_D^i}{D_e^{ij}} - \frac{N_D^i}{D_K^i} = \frac{p^i \nabla Y^i}{ZRT} + \left(1 + \frac{kp}{\mu_G D_K^i}\right)\frac{Y^i \nabla p^i}{ZRT} \tag{2.31}$$

where N^i_D is the molar flux of component g^i [mole m^{-2}s^{-1}], D_e^{ij} is the effective gas (binary) diffusivity of species g^i in species g^j, and $D_K^{\ i}$ is the Knudsen diffusivity of species g^i.

2.9. Salinity Effects on the Properties of the Aqueous Phase

The effects of salinity on the properties of the aqueous phase are fully described in the supplemental code unit **`T_Saliity_Effects.f95`** of TOUGH+ v1.5. Thus, the effect on the viscosity is described using correlations developed by *Phillips et al*. [1981] and by *Mao and Duan* [2009]. The effect on the density of the aqueous phase (brine) is computed from either an estimate of the critical brine saturation [*Sourirayan and Kennedy*, 1962] and the brine compressibility correlations of *Andersen et al*. [1992], or from the equations proposed by *Driesner* [2007]. The brine enthalpy is estimated using one of the following methods/options: *Michaelides* [1981], *Miller* [1978], *Lorenz* [2000] or *Driesner* [2007].

The effect of salinity on the vapor pressure is quantified by the relationships and process proposed by *Haas* [1976], and the salt concentration at the point of precipitation is estimated using the method of *Chou* [1987]. In both computations, the more accurate (but also far more computationally intensive) equations of *Driesner and Heinrich* [2007] were not implemented because *Battistelli* [2012] had already demonstrated that the deviations from the simpler equations were minimal to practically negligible in the range of temperatures of interest of the intended applications of the **T+RGB** code, i.e., for temperatures up to 450 ºC [*Battistelli*, 2012]. The halite density and enthalpy are computed using either (a) the correlations (default) of *Silvester and Pitzer* [1978] or (b) the fast parametric relationships of equations [*Battistelli*, 2012] that have been derived from the corresponding complex expressions of *Driesner* [2007]. The thermal conductivity of halite is described by the relationship of *Yang* [1981].

The computational process to estimate these properties is quite involved, and falls beyond the scope of this report. The interested user is directed to the publications of these authors for a detailed description of their methods.

2.10. Other Processes, Properties, Conditions, and Related Numerical Issues

All other processes needed to complete the description of the fluid flows and system behavior in gas-bearing geologic media are common to most problems of flow and heat flow through porous/fractured media, are fully covered in the description of the core TOUGH+ code [*Moridis*, 2014], and will not be repeated here. These include issues related to relative permeability, capillary pressure, treatment of fractured media, as well as the space and time discretization, the Newton-Raphson method and the use of the Jacobian in the fully implicit solution of these problems (the standard approach in all TOUGH+ applications). The interested reader is directed to *Moridis and Pruess* [2014] for a detailed discussion of all these subjects.

3.0. Design and Implementation of the T+RGB Code

3.1. Primary Variables

The thermodynamic state and the distribution of the mass components among the two or three possible phases are determined from the gas + H_2O + salt equation of state. Following the standard approach employed in the TOUGH2 [*Pruess et al.*, 1999; 2012] family of codes, in **T+RGB** the system is defined uniquely by a set of N_κ primary variables (where κ denotes the number of mass and heat components under consideration, see Section 2.2) that completely specifies the thermodynamic state of the system.

Although the number N_κ of the primary variables is initially set at the maximum expected in the course of the simulation and does not change during the simulation, the thermodynamic quantities used as primary variables can change in the process of simulation to allow for the seamless consideration of emerging or disappearing phases and components.

A total of 3 states (phase combinations) covering the entire possible phase if T > 0.01 ^{o}C and salt is not present are described in **T+RGB**; the number increases to 6 states when salinity is considered. The primary variables used for the various phase states without salt are listed in **Tables 3.1** and **3.2**, respectively. For systems with salinity, the additional primary variable is *X_s_A*, (corresponding to X_A^s, i.e., the mass fraction of salt in the aqueous phase). The primary variables in **Tables 3.1** and **3.2** are necessary and sufficient to uniquely define the H_2O-gas mixture-salt system.

3.2. Compiling the T+RGB Code

T+RGB is written in standard FORTRAN 95/2003. It has been designed for maximum portability, and runs on any computational platform (Unix and Linux workstations, PC, Macintosh) for which such compilers are available. Running **T+RGB** involves compilation and linking of the following code units and in the following order:

(1) **`T_RealGasBrine_Definitions.f95 (*)`**
Code unit providing default parameter values describing the basic attributes of the equation of state (i.e., number of components, number of phases, etc.)

(2) **`T_Allocate_Memory.f95`**
Code unit responsible for the dynamic memory allocation (following input describing the size of the problem) and dimensioning of most arrays needed by the code, in addition to memory deallocation of unnecessary arrays.

Table 3.1. Primary Variables in T+RGB Simulations Without Salt

Phase	State Identifier	Primary Variable 1	Primary Variables 2, … , N_G	Primary Variable N_G+1	Primary Variable N_G+2 (*)
1-Phase: G	**Gas**	*P_gas*	*Y_i_G, i=1,…,N_G-1*	*Y_N_G_G*	*T*
1-Phase: A	**Aqu**	*P*	*X_i_A, i=1,…, N_G-1*	*X_N_G_G*	*T*
2-Phase: A+G	**AqG**	*P_gas*	*Y_i_G, i=1,…,N_G-1*	*S_gas*	*T*

The possible primary variables are: *P*, pressure [Pa]; *P_gas*, gas pressure [Pa]; *T*, temperature [C]; *X_i_A*, mass fraction of gas *i* (*i*=1,…,N_G) dissolved in the aqueous phase [-]; *Y_ i_A*, mass fraction of gas *i* (*i*=1,…,N_G) dissolved in the aqueous phase [-]; *S_aqu*, liquid saturation [-]

$N_E = N_G+2$: maximum possible number of equations.

*For non-isothermal simulations only. For isothermal simulations, *T* is used to compute the thermophysical properties but is not part of the solution vector (i.e., the heat balance equation is not solved).

Table 3.2. Primary Variables in T+RGB Simulations With Salt

Phase	**State Identifier**	**Primary Variable 1**	**Primary Variables 2, … , N_G+1**	**Primary Variable N_G+2**	**Primary Variable N_G+3 (*)**
1-Phase: G	**Gas**	*P_gas*	*Y_i_G, i=1,…,*N_G	*X_s_G*	*T*
1-Phase: A	**Aqu**	*P*	*X_i_A, i=1,…,* N_G	*X_s_A*	*T*
2-Phase: A+G	**AqG**	*P_gas*	*Y_i_G, i=1,…,*N_G*-1, S_gas*	*X_s_A*	*T*
2-Phase: A+H	**AqH**	*P*	*X_i_A, i=1,…,* N_G	*S_aqu*	*T*
2-Phase: H+G	**GsH**	*P_gas*	*Y_i_G, i=1,…,*N_G	*S_gas*	*T*
3-Phase: A+H+G	**AGH**	*P_gas*	*Y_i_G, i=1,…,*N_G*-1, S_aqu*	*S_gas*	*T*

The possible primary variables are: *P*, pressure [Pa]; *P_gas*, gas pressure [Pa]; *T*, temperature [C]; *X_i_A*, mass fraction of gas *i* (*i*= 1,…, N_G) dissolved in the aqueous phase [-]; *Y_i_G*, mass fraction of gas *i* (*i* = 1,…, N_G) dissolved in the gas phase [-]; *S_aqu*, liquid saturation [-]; *S_gas*, gas saturation [-]; *X_s_A*, salt mass fraction in the aqueous phase [-].

$N_E = N_G+3$: maximum number of possible equations

*For non-isothermal simulations only. For isothermal simulations, *T* is used to compute the thermophysical properties but is not part of the solution vector (i.e., the heat balance equation is not solved).

(3) `T_Utility_Functions.f95`

Code unit that includes utility functions, i.e., a wide variety of mathematical functions, table interpolation routines, sorting algorithms, etc.).

(4) `T_H2O_Properties.f95`

Code unit that includes (a) all the water-related constants (parameters), and (b) procedures describing the water behavior and thermophysical properties/processes in its entire thermodynamic phase diagram.

(5) `T_Media_Properties.f95`

Code unit that describes the hydraulic and thermal behavior of the geologic medium (porous or fractured), i.e., capillary pressure and relative permeability under multiphase conditions, interface permeability and mobility, and interface thermal conductivity.

(6) `T_RealGas_Properties.f95 (#)`

Code unit that includes (a) the important constants (parameters) that are needed for the estimation of the properties of the various gases (see below), and (b) procedures describing the equation of state (EOS) of real gases (pure or mixtures) using any of the Peng-Robinson, Redlich-Kwong, or Soave-Redlich-Kwong cubic EOS model. The procedures in this code unit compute the following parameters and processes: compressibility, density, fugacity, enthalpy (ideal and departure), internal energy (ideal and departure), entropy (ideal and departure), thermal conductivity, viscosity, binary diffusion coefficients, solubility in water, and heat of dissolution in water.

(7) `T_Salinity_Effects.f95 (#)`

Code unit that computes all necessary properties and parameters in application options that involve salinity (e.g., brines). It estimates the salt solubility in H_2O, the halite density and enthalpy, the effect of salinity on the density, viscosity and enthalpy of the aqueous phase, as well as on the vapor pressure of H_2O.

(8) `T_NonDarcian_Flow.f95 (#)`

Code unit that computes all parameters and variables needed for the application of non-Darcian flow through porous and fractured media by accounting for inertial (turbulent) or viscous (slippage) effects. Thus, this unit reads all the non-Darcian flow inputs, and then uses them to compute all the parameters of the turbulent flow options (*Forcheimer* [1901] or *Barre and Conway* [2007]), of slippage flow (Klinkenberg flow [*Klinkenberg*, 1941], Knudsen diffusion [*Freeman et al*., 2011] or the Dusty Gas Model [*Mason and Malinauskas*, 1983; *Webb*, 1998]).

(9) `T_Geomechanics.f95`

Code unit that describes the geomechanically-induced changes on the flow properties of the porous media. These include porosity ϕ changes caused by pressure and/or temperature variations, intrinsic permeability k changes caused by porosity changes, and scaling of capillary pressures P_{cap} to reflect changes in ϕ and k. The ϕ and k changes are computed using either simplified of full geomechanical models. When the simplified model is invoked, ϕ is a function of (a) P and the pore compressibility α_P and (b) of T and the pore thermal expansivity α_T, while (c) k changes are estimated using empirical relationships (see Section 8). Changes in ϕ and k can also be computed by using a full geomechanical model, which can be optionally coupled with TOUGH+.

(10) `T_RealGasBrine_Specifics.f95 (*)`

Code unit that includes procedures specific to the **T+RGB** simulation, such as the reading of T+RGB-specific inputs, the preparation of the case-specific output files, the computation of the maximum amount of gas dissolved in the aqueous phase in the presence of salt, the computation of the sorbed gas masses, etc.. Generic procedures and operator extension – which override (*overload*) the standard procedures used by TOUGH+ for the simulation of general problems – are defined in this code unit, which does not include any procedures describing the gas + H_2O + salt equation of state.

(11) `T_Main.f95`

Main program that organizes the calling sequence of the high-level events in the simulation process, and includes the writing of important general comments in the standard output files, timing procedures, and handling of files needed by the code and/or created during the code execution.

(12) `T_RealGasBrine_EOS.f95 (*)`

Code unit that describes all the equations of state of the system, assigns initial conditions, computes the flow and thermophysical properties of the fluids, computes the flow properties of the medium, and determines phase changes and the state of the system from the possible options (see Section 3.1). This code unit also includes the procedure that computes the elements of the Jacobian matrix for the Netwon-Raphson iteration.

(13) `T_Matrix_Solvers.f95`

A linear algebra package that includes all the direct and iterative solvers available in TOUGH+ (see *Moridis and Pruess* [2014]).

(14) `T_Executive.f95`

The executive code unit of TOUGH+. It includes the procedures that advance the time in the simulation process, estimate the time-step size for optimum performance, populate the matrix arrays and invoke the solvers of the Jacobian, invoke special linear algebra for matrix pre-processing in cases of very demanding linear algebra problems, compute mass and energy balances, compute rates in sources and sinks, compute binary diffusion coefficients, write special output files, and conduct other miscellaneous operations.

(15) `T_Inputs.f95`

This code unit includes the procedures involved in the reading of the general input files needed for TOUGH+ simulations. It does not include any procedure reading T+RGB-related data (this is accomplished in the **`T_RealGasBrine_Specifics.f95`** code unit).

The code units denoted by (*) are specific to the **T+RGB** problem. The code unit denoted by (#) is not part of core TOUGH+ code but of the wider supplemental TOUGH+ code ensemble [*Moridis*, 2014], and is invoked to carry out the computations related to the system behavior needed by the REALGASBRINE v1.0 application option. All other code units are common to all TOUGH+ simulations.

Additionally, **T+ RGB** is distributed with the **`Meshmaker.f95`** FORTRAN code, which used to be part of the main code in the TOUGH2 simulators [*Pruess et al*., 1999; 2012], but is a separate entity in the TOUGH+ family of codes. **`Meshmaker.f95`** is used for the space discretization (gridding) of the domain of the problem under study (see *Moridis and Pruess* [2014]).

NOTE: In compiling **T+RGB** , *it is important that the free-format source code option be invoked for proper compilation of the FORTRAN 95/2003 code.*

4.0. Input Data Requirements

In this section, we discuss in detail mainly the input requirements that are specific to the needs of the REALGASBRINE v1.0 application option. All inputs that are generic in type and common to any simulation of flow and transport through porous media are fully described in *Moridis and Pruess* [2014] and will not be repeated here. The reader is directed to the *Moridis and Pruess* [2014] report for details on the description of all such inputs and on the structure of the input files. Note that, to ensure backward compatibility with input files from older simulations, some input data for **T+RGB** simulations conform to older formats. The data inputs to activate the new capabilities in TOUGH+ v1.5 and REALGASBRINE v1.0 follow more advanced formats such as namelists.

Some of these non-EOS specific data are also discussed here (in essence, repeating the information in *Moridis and Pruess* [2014]) for additional emphasis, as these *may* play an important role in **T+RGB** simulations. Unless otherwise indicated, all input data are in standard metric (SI) units, such as meters, seconds, kilograms, ˚C and in the corresponding derived units, such as Newtons, Joules, Pascal (= N/m^2 for pressure), etc.

4.1. Input Data Blocks

In the **T+RGB** input files, data are organized in standard TOUGH2 and TOUGH+ structure that involves data blocks that are defined by keywords. **Table 4.1** provides a listing and a short description of all the data blocks (mandatory and optional) in a **T+RGB** input file. Note that, as a result of the modular structure of the TOUGH+ architecture [*Moridis*, 2014], only a single data block (**`REAL_GAS+H2O`** or **`REAL_GAS+H2O`**) is specific to this application option, and all other ones are generic and common to any TOUGH+ simulation.

4.2. Data Block **`MEMORY`**

This block is a mandatory component of the generic TOUGH+ input file, and is discussed here only in order to provide a list of values for the parameters needed for an appropriate allocation of the dynamic memory. Thus, the following options are possible:

`binary_diffusion` `=.TRUE.` if diffusion is considered
`=.FALSE.` if diffusion is ignored

The following combinations are possible for **T+RGB** simulations:

(1) `(NumCom, NumEq, NumPhases) =` $(N_G+1,N_G+1,2)$:
Water, real gas mixture, no salt, isothermal

(2) `(NumCom, NumEq, NumPhases) =` $(N_G+1,N_G+2,2)$:
Water, real gas mixture, no salt, non-isothermal

Table 4.1. Input data blocks for a T+RGB simulation

Keyword (+)	***Sec.* (#)**	***Function***
TITLE (1st record)	4.1.1	Data record (single line) with simulation title
MEMORY (2nd record)	5.1	Dynamic memory allocation
REAL_GAS+H2O or **REAL_GAS+Brine**	4.2(^)	Parameters describing the case-specific T+RGB system properties
ROCKS or **MEDIA**	6.2	Hydrogeologic parameters for various reservoir domains
RPCAP or **WETTA**BILITY	6.3	Optional; parameters for relative permeability and capillary pressure functions
DIFFUSION	6.4	Optional; diffusivities of mass components
***ELEME**	7.1	List of grid blocks (volume elements)
***CONNE**	7.2	List of flow connections between grid blocks
INDOM	8.1	Optional; initial conditions for specific reservoir domains
***INCON**	8.2	Optional; list of initial conditions for specific grid blocks
EXT-INCON	8.3	Optional; list of initial conditions for specific grid blocks
BOUNDARIES	8.6	Optional; provides time-variable conditions at specific boundaries
***GENER**	9.1	Optional; list of mass or heat sinks and sources
PARAM	10.1	Computational parameters; time stepping and convergence parameters; program options
SOLVR	10.2	Optional; specifies parameters used by linear equation solvers.
TIMES	11.2	Optional; specification of times for generating printout
SUBDOMAINS	11.3	Optional; specifies grid subdomains for desired time series data
INTERFACES	11.4	Optional; specifies grid interfaces for desired time series data
SS_GROUPS	11.5	Optional; specifies sink/source groups for desired time series data
ENDCY (last record)	4.1.3	Record closes TOUGH+ input file and initiates simulation
ENDFI (last record)	4.1.4	Alternative for closing TOUGH+ input file which causes flow simulation to be skipped.

#: Denotes the section number in the *Moridis and Pruess* [2014] report
^: Denotes the section number in this report
*: Data can be provided as separate disk files and omitted from input file.
+: The bold face part of the keyword (left column) suffices for data block recognition

(3) `(NumCom, NumEq, NumPhases) = (`N_G`+2,`N_G`+2,3):`
Water, real gas mixture, salt, isothermal

(4) `(NumCom, NumEq, NumPhases) = (`N_G`+2,`N_G`+3,3):`
Water, real gas mixture, salt, non-isothermal

Any value of the `NumCom, NumEq, NumPhases` parameters other than those described here results in an error message and the cessation of the simulation. The selection of appropriate values for all other variables in this data block is left to the user.

4.3. Data Block `ROCKS` or `MEDIA`

The discussion here is limited to the specific parameters that *may be* needed in a **T+RGB** simulation. Information on all the other parameters in the specified records is found in *Moridis and Pruess* [2014].

Record `ROCKS.1`

`NAD` = `8`: In addition to the standard four records read for NAD > 2, an additional (fifth) record will be read with information on the whether slippage and inertial/turbulent flow effects will be considered in this medium.

Record `ROCKS.1.4`

Optional, for NAD = `8` only. This record includes general data describing whether non-Darcian flow is to be considered in this medium. The namelist in this record is named `Slippage_Turbulence_Info`, and has the following general form:

```
&Slippage_Turbulence_Info  MediumKnudsenFlow_F     = .x.,
                           MediumTurbulentFlow_F   = .x.,
                           MediumKlinkFlow_F       = .x.,
                           Option_KlinkenbergParam = 'x'
                           /
```

The parameters in the namelist `NonDarcian_Flow_Specifications` are defined as follows:

`MediumKnudsenFlow_F`
A logical parameter indicating whether Knudsen diffusion will be considered in this medium. The possible values are `.TRUE.` or `.FALSE.`

`MediumTurbulentFlow_F`

A logical parameter indicating whether turbulent flow will be considered in this medium. The possible values are `.TRUE.` or `.FALSE.`

`MediumKlinkFlow_F`

A logical parameter indicating whether Klinkenberg flow (gas slippage) will be considered in this medium. The possible values are `.TRUE.` or `.FALSE.`

`Option_KlinkenbergParam`

A character parameter of length `LEN = 5` defining the method to be used for the estimation of the slippage parameter *b*. The following options are available:

`='CON'`: The *b* value provided in the data block **ROCKS** (see *Moridis and Pruess* [2014]) is used.

`='FIXED'`: The *b* value is obtained as a function of the initial intrinsic permeability *k* from interpolation in a table provided by *Wu et al.* [1988] and remains fixed during the simulation (default).

`='C-INT'`: The *b* value is obtained as a function of the **initial (constant)** *k* from interpolation in a table provided by *Wu et al.* [1988] and varies with *k* during the simulation.

`='V-INT'`: The *b* value is obtained as a function of the **variable** *k* (changing during the simulation as a result of changing *P* and *T*) from interpolation in a table provided by *Wu et al.* [1988] and varies with *k* during the simulation.

`='C-REF'`: The *b* value is obtained as a function of a reference **constant** *k* using the method of *Jones* [1972] and interpolation in a table provided by *Wu et al.* [1988].

`='V-REF'`: The *b* value is obtained as a function of a reference **variable** *k* (changing during the simulation as a result of changing *P* and *T*) using the method of *Jones* [1972] and interpolation in a table provided by *Wu et al.* [1988].

`='C-JOW'`: The *b* value is obtained as a function of a reference **constant** (**initial**) *k* using the method of *Jones and Owens* [1979].

`='V-JOW'`: The *b* value is obtained as a function of a reference **variable** *k* (changing during the simulation as a result of changing *P* and *T*) using the method of *Jones and Owens* [1979].

`='C-SAK'`: The *b* value is obtained as a function of a reference **constant** (**initial**) *k* and ϕ using the method of *Sampath and Keighin* [1981].

`='V-SAK'`: The *b* value is obtained as a function of a reference **variable** *k* (changing during the simulation as a result of changing *P* and *T*) and ϕ using the method of *Sampath and Keighin* [1981].

`='C-FLO'`: The *b* value is obtained as a function of a reference **constant** (**initial**) *k* and *b* using the method of *Florence* [1988].

`='V-FLO'`: The *b* value is obtained as a function of a reference **variable** *k* (changing during the simulation as a result of changing *P* and *T*) and ϕ using the method of *Florence* [1988].

4.3. Data Block `REAL_GAS+H2O` or `REAL_GAS+Brine`

The parameters describing the system properties and behavior are provided here. Note that namelist-based format is used to read the data in this data block. This is a very powerful format that allows maximum clarity and flexibility, accepting free formats, arbitrary ordering of variables, insertions of comments anywhere in the input fields, and providing the option of ignoring any of the `NAMELIST` parameters by not assigning a value to it. For more information, the reader is directed to a textbook on FORTRAN 95/2003.

Record `TRGB.1`

This record includes general data describing whether non-Darcian flow is to be considered. The namelist in this record is named `NonDarcian_Flow_Specifications`, and has the following general form:

```
&NonDarcian_Flow_Specifications
                    turbulent_flow_F       = .x.,
                    turbulent_phase_flow_F = .x.,
                    Option_turbulent_FlowEquation = 'x ',
                    Option_turbulent_FlowEqParam  = 'x ',
                    Knudsen_diffusion_F = .x.,
                    slippage_effects_F  = .x.,
                    dusty_gas_model_F   = .x.,
                    /
```

The parameters in the namelist `NonDarcian_Flow_Specifications` are defined as follows:

`turbulent_flow_F`

A logical parameter indicating whether turbulent flow will be considered at all. The possible values are `.TRUE.` or `.FALSE.`

`turbulent_phase_flow_F`

A logical array of dimension `NumMobPhases` indicating whether flow of any of the mobile phases is turbulent flow. The possible values of each array element are `.TRUE.` (mainly for the gas phase) or `.FALSE.` (usually for the aqueous phase).

`Option_turbulent_FlowEquation`

A character parameter of length 5 defining the type of turbulent flow equation to be used. The following options are available:

=`'FORCH'`: This option invokes the *Forchheimer* [1901] equation for turbulent flow.

=`'BARCO'`: The *Barree and Conway* [2007] equation is used.

`Option_turbulent_FlowEqParam`

A character parameter of length 3 defining the method to compute the parameters for the chosen turbulent flow equation to be used. The following options are available:

=`'CON'`: A constant value is used for the parameter $\beta_{F\beta}$ of the *Forchheimer* [1901] equation for turbulent flow.

=`'LIU'`: This option invokes the *Forchheimer* [1901] equation for turbulent flow.

=`'G'`: The method of *Geertsma* [1974] is used (default).

=`'JK'`: The method of *Janicek and Katz* [1955] is used.

=`'FG3'`: The method of *Frederick and Graves* [1994], Eq. 3 is used.

=`'FG4'`: The method of *Frederick and Graves* [1994], Eq. 4 is used.

=`'FG5'`: The method of *Frederick and Graves* [1994], Eq. 5 is used.

=`'FG6'`: The method of *Frederick and Graves* [1994], Eq. 6 is used.

=`'LIU'`: The method of *Liu et al.* [1995] is used.

=`'TM'`: The method of *Thauvin and Mohanty* [1998] is used.

=`'CM'`: The method of *Coles and Hartman* [1998] is used.

=`'C'`: The method of *Cooper et al.* [1999] is used.

=`'E'`: The method of *Ergun* [1952] is used.

`Knudsen_diffusion_F`

A logical parameter indicating whether Knudsen diffusion will be considered at all. The possible values are `.TRUE.` or `.FALSE.`

`slippage_effects_F`

A logical parameter indicating whether slippage effects (Klinkenberg flow) will be considered at all. The possible values are `.TRUE.` or `.FALSE.`

`dusty_gas_model_F`

A logical parameter indicating whether the dusty gas model [*Webb*, 1998] will be considered at all. The possible values are `.TRUE.` or `.FALSE.`

Record `TRGB.2`

This record includes general data describing key diffusion parameters. The namelist in this record is named `Gas_Specifications`, and has the following general form:

```
 &Gas_Specifications  number_of_component_gases   = x,
                      component_gas_name          ='x',…, 'x',
                      component_gas_mole_fraction = x,…,x
                      gas_cubic_EOS = 'x',
                      sorbed_gas_F  = .x.,
                      variable_gas_composition_F = .x.,
                      gas_viscosity_equation = 'x…x'
                      gas_DepEnthalpy_equation = 'x…x'
                      /
```

The parameters in the namelist `NonDarcian_Flow_Specifications` are defined as follows:

`number_of_component_gases`

An integer parameter specifying the number of gases; water may be omitted, as it is automatically added by the code.

`component_gas_name`

A character array of length 6 and of dimension `number_of_component_gases` describing the names of the gases. The possible options are:

`'CH4'`, `'C2H6'`, `'C3H8'`, `'nC4H10'`, `'nC4H10'`, `'H2O'`, `'CO2'`, `'H2S'`, `'O2'`, `'N2'`, `'C2H5OH'` and `'H2'`

`component_gas_mass_fraction`

A real array of dimension `number_of_component_gases` describing the mole fractions of the gases in the initial gas mixture.

`gas_cubic_EOS`

A character parameter of length 3 defining the type of the cubic equation-of-state (EOS) to be used for the gas mixture. The following options are available:

=`'PR'`: This option invokes the *Peng and Robinson* [1976] equation for turbulent flow (default).

=`'SRK'`: The *Soave* [1972] equation is used.

=`'RK'`: The *Redlich and Kwong* [1949] equation is used.

`sorbed_gas_F`

A logical parameter indicating whether gas sorption will be considered at all. The possible values are `.TRUE.` or `.FALSE.`

`variable_gas_composition_F`

A logical parameter indicating whether the dry gas will be treated as a constant-composition pseudo-component (=`.FALSE.`), or if its constituent gases will be tracked individually (=`.TRUE.`).

`gas_viscosity_equation`

A character variable of maximum length `LEN = 10` that describes the name of the gas viscosity equation to be used. *Only the first character of the equation name is important*, so the first letter is sufficient to define the equation. The available options are:

=`'`**`Q`**`uinones'`: The *Quinones et al.* [2000] friction theory (*f*-theory) equation is used (default).

=`'`**`C`**`hung'`: The *Chung et al.* [1988] viscosity equation is used.

NOTE: *Any equation name different from the ones listed above (including a blank or no specification at all in the namelist) is automatically reset to* `'`**`C`**`'`. *The Chung method MUST be used if the gas includes hydrogen H_2.*

`gas_DepEnthalpy_equation`

A character variable of maximum length `LEN = 10` that describes the name of the equation used to compute the departure enthalpy of the real gas mixture under investigation. *Only the first character of the equation name is important*, so the first letter is sufficient to define the equation. The available options are:

=`'`**`C`**`EOS'`: The departure enthalpy is computed using the relationships associated with the cubic equation of state defined by the `gas_cubic_EOS` *parameter* (default).

=`'`**`L`**`eeKesler'`: The Lee-Kesler 5th order equation of state [*Lee and Kesler*, 1975] is used. This equation is recommended for gas mixtures involving large amounts of hydrocarbons and CO_2 because of its superiority over the standard cubic EOS for such calculations.

NOTE: *Any equation name different from the ones listed above (including a blank or no specification at all in the namelist) is automatically reset to* `'C'`.

Record `TRGB.3`

This record is needed only if `sorbed_gas_F = .TRUE.`, is named `Sorption_Specifications`, its function is self-explanatory, and has the following general form:

```
 &Gas_Specifications  medium_name             = 'x',
                      medium_number           =  x,
                      sorbing_comp_name       = 'x'
                      sorbing_comp_number     =  x,
                      sorption_equation_name = 'x',
                      sorption_parameters     =  x,…,x
                      /
```

The parameters in the namelist `NonDarcian_Flow_Specifications` are defined as follows:

`medium_name`
A character parameter of length 5 specifying the name of the sorbing rock (see data block **ROCKS** in *Moridis and Pruess* [2014]).

`medium_number`
An integer parameter specifying the number of the sorbing rock in the listing sequence (see data block **ROCKS** in *Moridis and Pruess* [2014]). Either the name or the number of the sorbing rock is sufficient.

`sorbing_comp_name`
A character parameter of length 6 specifying the name of the sorbing gas component (see record `TRGB.2` above).

`sorbing_comp_number`
An integer parameter specifying the number of the number of the sorbing in the listing sequence (see record `TRGB.2` above).

`component_gas_name`
A character array of length 6 and of dimension `number_of_component_gases` describing the names of the gases. The possible options are: `CH4, C2H6, C3H8, nC4H10, nC4H10, H2O, CO2, H2S, O2, N2, C2H5OH` and `H2`

`component_gas_mass_fraction`
A real array of dimension `number_of_component_gases` describing the mole fractions of the gases in the initial gas mixture.

`sorption_equation_name`

A character parameter of length 10 specifying the name of the sorption equation for the specified rock and spesies. The options are:

='EQU-LANG-B' or 'EQU-LANG-B': Equilibrium Langmuir sorption

='KLAS': Kinetic Langmuir sorption

='ELIS': Equilibrium linear sorption

='KLIS': Kinetic linear sorption.

='EFS': Equilibrium Freundlich sorption

='KFS': Kinetic Freundlich sorption.

`sorption_parameters`

A real array of dimension 6 listing the parameters of the sorption equation.

Record `TRGB.4`

This record is needed only if the data block name is **`REAL_GAS+BRINE`**, is named `Brine_Specifications`, its function is self-explanatory, and has the following general form:

```
 &Brine_Specifications
              brine_viscosity_computation_method = 'x',
              brine_density_computation_method   = 'x'/
              brine_enthalpy_computation_method  = 'x'/
              halite_density_computation_method  = 'x'/
              halite_enthalpy_computation_method = 'x'/
```

The parameters in the namelist `Brine_Specifications` are defined as follows:

`brine_viscosity_computation_method`

A character parameter of length 3 specifying the method to compute the brine viscosity. The possible options are:

='PHI' or blank or any 3 character-word: The method of *Phillips et al.* [1981] is used (DEFAULT)

='MAO': The method of *Mao and Duan* [2009]

`brine_density_computation_method`

A character parameter of length 3 specifying the method to compute the brine density. The possible options are:

`='SKA'` or blank or any 3 character-word: A method based on the critical pressure of *Sourirayan and Kennedy* [1962] and the compressibility approach of *Andersen et al.* [1992] is used (DEFAULT)

`='DRI'`: The method of *Driesner* [2007]

`brine_enthaly_computation_method`
A character parameter of length 3 specifying the method to compute the brine enthalpy. The possible options are:

`='LOR'` or blank or any 3 character-word: The method of *Lorenz* [2000] is used (DEFAULT)

`='MIC'`: The method of *Michaelides* [1981]

`='MIL'`: The method of *Miller* [1978]

`='DRI'`: The method of *Driesner* [2007]

`halite_density_computation_method`
A character parameter of length 3 specifying the method to compute the halite density. The possible options are:

`='S&P'` or blank or any 3 character-word: A method based on the approach of *Silvester and Pitzer* [1972] is used (DEFAULT)

`='D&H'`: The method of *Driesner and Heirich* [2007]

`halite_enthaly_computation_method`
A character parameter of length 3 specifying the method to compute the halite enthalpy. The possible options are:

`='S&P'` or blank or any 3 character-word: A method based on the approach of *Silvester and Pitzer* [1972] is used (DEFAULT)

`='B&D'`: The *Battistelli* [2012] parametric correlation of the *Driesner* [2007] equation

4.5. Data Block `DIFFUSION`

This block reads multicomponent diffusion coefficients using a `NAMELIST` format. This is a very powerful format that allows maximum clarity and flexibility, accepting free formats, arbitrary ordering of variables, insertions of comments anywhere in the input fields, and providing the option of ignoring any of the `NAMELIST` parameters by not assigning a value to it. For more information, the reader is directed to a textbook on FORTRAN 95/2003.

In **T+RGB** applications, this capability may be invoked in long-term studies (covering multi-year periods). Diffusion is not expected to play a significant role in the course of most cases of production from gas-bearing geologic media because, in such a case, advective effects constistently overwhelm diffusive transport.

Record `DIFFUSION.1`

This record includes general data describing key diffusion parameters. The namelist in this record is named `Diffusion_Key_Parameters`, and has the following general form.

```
&Diffusion_Key_Parameters
     gas_diffusivity_equation_exponent  = x.xEx,
     P_at_RefDiffusivity                = x.xEx,
     Tk_at_RefDiffusivity               = x.xEx
     full_multiphase_diffusion          = .x
                                        /
```

The parameters in the namelist `Diffusion_Key_Parameters` are defined as follows:

`gas_diffusivity_equation_exponent`
A double precision variable describing the dependence of gas diffusivity on temperature (see Equation 6.4 in *Moridis and Pruess* [2014]). The default value is 1.80.

`P_at_RefDiffusivity`
Pressure at the reference diffusivity (in Pa). If `P_at_RefDiffusivity <= 0`, the default value is 10^5 Pa.

`Tk_at_RefDiffusivity`
Temperature at the reference diffusivity (in K). If `T_at_RefDiffusivity <= 0`, the default value is 273.15 K.

`Option_gas_diffusivity_CompuMethod`
A character variable describing the method of estimation of the binary **gas** diffusivities. The following options are available:

`='Standard'`: This option involves the application of Equation (6.4) in *Moridis and Pruess* [2014], and requires non-zero multicomponent gas diffusivity values read from the standard input file.

`='Real_Gas_EOS'`: In this case, the binary gas diffusivities are computed from the cubic equation of state used to determine all the real gas properties. The diffusivities in the aqueous phase still need to be provided.

`='Constant'`: When this option is invoked, the constant multicomponent diffusivity values provided in the input file are used.

`full_multiphase_diffusion`

A logical variable describing the method of estimation of the method of estimation of multiphase diffusive fluxes. The following options are available:

`=.TRUE.`: With this option, harmonic weighting to the full multiphase effective diffusion strength is applied. This includes contributions from gas and aqueous phases, accounts for coupling of diffusion with phase partitioning effects, and can describe the most general cases of diffusion across phase boundaries.

`=.FALSE.`: In this case, harmonic weighting is performed separately for the diffusive fluxes in the mobile phases.

Records `DIFFUSION.2.1`, `DIFFUSION.2.2`, etc.

Record `DIFFUSION.2.1` is followed by `DIFFUSION.2.x` records, with `x = 1,…,NubMobPhases` (i.e., the number of mobile phases in the system under study). These records describe component diffusivities in the various phases. The same namelist is used in each one of these records. It is named

`Component_Diffusivities_in_Phases`

and has the following general form:

```
&Component_Diffusivities_in_Phases
     phase        = x,
     phase_number = x,
     component(1) = x,
          component_number(1)      = x,
          component_diffusivity(1) = x.xEx,
     component(2) = x,
          component_number(2)      = x,
          component_diffusivity(2) = x.xEx,
     …
     …
     …
     /
```

The parameters in the namelist `Diffusion_Key_Parameters` are defined as follows:

`phase`

A character variable identifying the mobile phase for which the diffusivities of the various components are reported. The possible options in the **T+RGB** code are '`Aqueous`' and '`Gas`'.

`phase_number`

An integer variable providing the number of the phase in the phase numbering sequence used in the code. The possible options in the **T+RGB** code are:
= `2` for `phase` = '`Aqueous`', and
= `1` for `phase` = '`Gas`'.

`component`

A character array of dimension `NumCom` (see Section 5.1) identifying the various mass components partioned in the phase in question (denoted by `phase`). The possible options in the **T+RGB** code are: '`CH4`', '`H2O`' and '`NaCl`' (if salinity is considered).

`component_number`

An integer array providing the number of the component in the numbering sequence used in the code. The possible options in the **T+RGB** code are:
= `1` for `component` = '`CH4`'
= `2` for `component` = '`H2O`'
= `3` for `component` = '`NaCl`' (if present)

`component_diffusivity`

A double precision array of dimension `NumCom` (see Section 5.1) describing the value of the multicomponent diffusivities D_β^κ (see Equations (2.59) and (6.4)) of the various components κ in the phase β under consideration (indentified by `phase` and `phase_number`, respectively).

NOTE: *The records* `DIFFUSION.2.x` *must provide data for all mobile phases and all components, even if the gas diffusivities may be overridden internally when* `Option_gas_diffusivity_CompuMethod = 'Real_Gas_EOS'`.

The structure of the namelists `Diffusion_Key_Parameters` and `Component_Diffusivities_in_Phases` (and their use as input formats in the data block **`DIFFUSION`**) are best illustrated in the example of **Figure 4.1**.

```
DIFFUSION-----*----2----*----3----*----4----*----5----*----6----*----7----*----8
&Diffusion_Key_Parameters  gas_diffusivity_equation_exponent  = 1.8d0
                           P_at_RefDiffusivity                = 1.0d5,    ! in Pa
                           Tk_at_RefDiffusivity               = 273.15d0, ! in K
                           Option_gas_diffusivity_CompuMethod = 'Real_Gas_EOS',
                           full_multiphase_diffusion          = .TRUE.
                           /
&Component_Diffusivities_in_Phases
        phase        = 'Aqueous',  phase_number = 2,
        component(1) = 'CH4',      component_number(1) = 1,
        component_diffusivity(1) = 1.0d-10,  ! (m2/s) ! Diffusivity of component 1 in phase 2
        component(2) = 'H2O',      component_number(2) = 2,
        component_diffusivity(2) = 1.0d-10,  ! (m2/s) ! Diffusivity of component 2 in phase 2
        component(3) = 'NaCl',     component_number(3) = 3,
        component_diffusivity(3) = 1.0d-10   ! (m2/s) ! Diffusivity of component 3 in phase 2
        /
&Component_Diffusivities_in_Phases
        phase        = 'Gas',      phase_number = 1,
        component(1) = 'CH4',      component_number(1) = 1,
        component_diffusivity(1) = 1.0d-05,  ! (m2/s) ! Diffusivity of component 1 in phase 1
        component(2) = 'H2O',      component_number(2) = 2,
        component_diffusivity(2) = 1.0d-05,  ! (m2/s) ! Diffusivity of component 2 in phase 1
        component(3) = 'NaCl',     component_number(3) = 3,
        component_diffusivity(3) = 0.0d-00   ! (m2/s) ! Diffusivity of component 3 in phase 1
        /
```

Figure 4.1. The **`DIFFUSION`** data block, with examples of the `Diffusion_Key_Parameters` and `Component_Diffusivities_in_Phases` namelists.

5. Outputs

In this section, the various primary and secondary variables that may be provided as outputs from **T+RGB** simulations are discussed. Such outputs are provided in the following cases:

- In the standard **T+RGB** output as an ASCII file either at selected times (defined in the data blocks `TIMES`), or at a given timestep frequency (defined by the variable `PRINT_frequency` in the data block `PARAM`, see *Moridis and Pruess* [2014]). The standard output provides information on all elements and connections in the grid of the system.
- In an output file named **`Plot_Data_Elem`**, which stores the element-specific properties and parameters in a format that conforms to the requirements of the TecPlot package [*TecPlot*, 2003], and is suitable for most other plotting and graphing packages. This file is printed when the variable `MOP(19)=8` for `9` in the

data block `PARAM` and provides information on all elements of the domain (see *Moridis and Pruess* [2014]). Note that for `MOP(19)=9`, the plotting file and a truncated standard output file are produced (listing only mass balances at the prescribed printout times).

- In output files named after each of the subdomains, interfaces or groups of sinks and sources (wells) defined in the data blocks `SUBDOMAINS`, `INTERFACES` and `SS_GROUPS`, respectively. These files provide time series of relevant data at a frequency determined by the input parameter `TimeSeries_frequency` in the in the data block `PARAM` (see *Moridis and Pruess* [2014]).

5.1. The Standard Outputs

The standard output of the **T+RGB** code provides the following output:

1. The pressure, temperature, phase saturations, gas partial pressure, H_2O vapor pressure, sorbed gas mass and salt mass fraction in all elements of the domain.

2. The mass fractions of the individual gases in the gas and aqueous phases, phase densities and viscosities, porosities, capillary pressure and relative permeabilities to the mobile phases.

3. The flows and velocities of the phases through the element interfaces (connections) of the domain; the corresponding flows of the gas constituents in the mobile phases (i.e., aqueous and gas), and the heat flow; the diffusive flows (if accounting for diffusion).

4. The primary variables and their changes in the elements of the domain.

5. The phase enthalpies, the temperature shift (when salt is present), the intrinsic permeabilities and the permeability-reduction factor in the presence of solid phases (if the EPM model is used, see *Moridis and Pruess* [2014]) in all elements of the domain.

6. Source and sink (well) information, including: mass and enthalpy rates, mobile phase mass fractions in the injection/production stream, gas and H_2O mass flow

rates in the mobile phases.

7. Volume and mass balances of the phases and components in the domain.

All the units of the various parameters are listed in the standard output file. Of the possible outputs, (1), (2), (6) and (7) are always printed in the standard **T+RGB** output. The amount of the additional output is controlled by the parameter `OutputOption` in the data block `PARAM`. Thus, (3) is printed in addition when `OutputOption = 2`, and a complete data set (items 1 to 7) is printed when `OutputOption = 3`. In keeping with the TOUGH2 [Pruess et al., 1999] and TOUGH + convention [*Moridis*, 2014], printouts occur after each iteration (not just after convergence) if the `OutputOption` values are increased by 10.

For `MOP(19)>7`, the **`Plot_Data_Elem`** file includes the following information: the coordinates of each element center in the domain, and the corresponding pressure, temperature, phase saturations, relative permeability of the mobile (aqueous and gas) phases, the capillary pressure, the component (gases, H_2O and salt) mass fractions in the various phases, the sorbed gas mass, permeability, porosity and the permeability-reduction factor in the presence of solid phases (meaningful only if the EPM model is invoked, see *Moridis and Pruess* [2014]).

5.2. Time Series Outputs

Time series outputs are obtained when the data blocks `SUBDOMAINS`, `INTERFACES` and `SS_GROUPS` are included in the **T+RGB** input files. Thus, individual output files are created for each one of the subdomains identified in `SUBDOMAINS` (see detailed discussion in *Moridis and Pruess* [2014]), and there the following data are written with a frequency defined by the parameter `TimeSeries_frequency`:

- The subdomain pore volume, and pore-volume averaged pressure, temperature, and gas saturation in the subdomain.
- The mass of each of the phases and of the salt (if present).
- The mass of the individual gases in the aqueous and the gas phase, and on the grains of the porous medium (sorbed).

Similarly, individual output files are created for each one of (a) the interfaces identified in `SUBDOMAINS` and (b) the source/sink (well) groups identified in `SS_GROUPS` (see detailed discussion in *Moridis and Pruess* [2014]), and there the following data are written with a frequency defined by the parameter `TimeSeries_frequency`:

- The mass flow rate of the mobile (aqueous and gas) phases across the interface or through the source/sink group, as well as the corresponding individual gas and H_2O flows in each of the mobile phases, the salt flow and the heat flow.
- The cumulative mass of each of the mobile (aqueous and gas) phases that flowed across the interface or through the source/sink group since the beginning of the simulation, as well as the corresponding mass of individual gas and H_2O in each of the mobile phases and the salt mass.

All the units (SI) of the various listed parameters are listed in the headings of the output file.

6.0. Example Problems

6.1. Example Files and Naming Conventions

The files corresponding to the examples discussed in this manual can be found in the directory `Test_Problems_TRBG_V1.0` in the USB memory stick accompanying this manual. The input files of the example problems are the following:

1. `Test1`
2. `Test2`
3. `Test3`
4. `Test4`
5. `Test5`
6. `ProblemV1`
7. `ProblemV2`
8. `ProblemV3`
9. `ProblemA1`

Of those, the ones with the '`ProblemV`' identifier are used to demonstrate the range of capabilities of the code. Those with the '`ProblemV`' identifier denote problems of validation of existing analytical solutions, and those with the '`ProblemA`' identifier denote larger application problems.

The corresponding output files are also included in the directory `"Test_Problems_TRBG_V1.0"` on the memory stick distributed during the class. The naming convention of the generic TOUGH+ output files involves the suffix `".out"` at the end of the input file name. For the case of **`Test1`**, some additional files that are created per the specifications of the output options in the input data files are also included. These have the user-defined names '**`WellZ_Time_Series`**', '**`IntRR_Time_Series`**' and '**`Wells_Time_Series`**' and (see input file **`Test1`** in the Appendix or on the memory stick), and represent time series of data at subdomain, through an interface and through a source/sink group, respectively.

6.2. Problem Test1: Single Gas Flow and H2O, Radial System, Gas, Non-Isothermal

This 1-D radial problem is designed to demonstrate the basic concepts of input file creation and structure, and to demonstrate the evolution of the state of a cylindrical reservoir in the course of production. The gas is 100% CH_4, there is no salt in the system, and the reservoir is initially at a 2-phase state with $S_A = 0.5$. This is a low-permeability system tight-sand system, which means that gas sorption onto the grains of the porous medium can is minimal and can be ignored. The simulation accounts for Knudsen diffusion, the parameters of which are computed internally using the equations discussed in Section 2.

As production continues, the pressure is expected to continuously decline, and the same is expected of the temperature because of the Joule-Thomson effect near the wellbore. Additionally, the pressure drop should also result in an increase in the apparent permeability of the system because of the increase in the mean travel path of the gas. Because all the physics are represented into the T+RGB code, this is expected to be a dynamic system, with all the fluid properties varying continuously.

For convenience, the input file is listed in **Figure 6.1**. As an exercise, a novice user is urged to identify the various variables and parameters in the input file.

The cylindrical domain (represented by 33 active cells of non-uniform radial increments and having a thickness of Δz = 10 m size) is a pressurized and thermally insulated reservoir of a porous medium, in which CH_4 and water coexist at a pressure of 10^7 Pa and T = 10 ^oC. At a time t = 0, production begins at three sinks (wells), one of which is located at the center of the cylindrical reservoir. The production rate is the same Q = 0.1 kg/sin all 3 wells. Note that, in a cylindrical system as the one described here (also known as single-well problems), it is next to impossible to have wells away from the center of the domain representing any real-life scenario, unless a large number of wells are installed on a circular pattern around the center well. However, here this is acceptable as a numerical exercise.

The porous medium has a porosity ϕ = 0.1, and a permeability $k = 3\text{x}10^{-15}$ m^2 (= 3 mD in oilfield units). Strictly speaking, this is not classified as a tight system, but this is not a problem because this sample problem is used for illustration purposes, and the permeability will be changed (and the problem rerun) during the training session. A non-zero pore compressibility (=10^{-9} 1/Pa, i.e., typical of sandstones) is assigned to the porous medium. This is necessary in hydrate simulations, in which evolution of solid phases of lower density (such as ice and hydrate) can lead to extraordinarily high pressures as the aqueous phase disappears if pore compressibility is small. The thermal conductivity (=3.1 W/m/K) is also typical of water-saturated sandstone media. The relative permeability is computed from the Modified Stone equation, and the relative permeability from the vanGenuchten equation (see *Moridis and Pruess* [2014])

`Test1.out`, the standard TOUGH+ output corresponding to the input file **`Test_1T`**, can be found in the directory `Test_Problems_TRBG_V1.0` in the USB memory stick accompanying this manual. Because `MOP(5) = 0`, the output does not includes detailed messages about the evolution of the residuals during the Newtonian iterations at each time step (phase changes are not possible in this system). Because `OutputOption = 3`, a full output is obtained that provides a very detailed list of the conditions, parameters and thermophysical properties of the system at each cell and at each connection. Thus, the output describes the pressure, temperature, phase saturation, partial CH_4, H_2O-vapor pressure, equilibrium hydration pressure, salt mass fraction in the aqueous phase, CH_4 concentrations in the aqueous and gas phases, phase densities, porosity, capillary pressure, relative permeability of the gas and aqueous phases, the amount of sorbed gas, heat and fluid fluxes, mobile phase velocities, CH_4 fluxes in the aqueous and gas phases, primary variables and their changes, phase enthalpies, the effect of Knudsen diffusion on the permeability, and the temperature shift in the hydrate P-T equilibrium caused by the presence of the inhibitor. Additionally, the output provides mass and volume balances of the phases, component mass balances, and component distribution into the phases.

The results in the portion of the output in the **`Test_1T.out`** file (see Appendix A) are consistent with the expected system response. Production at the central well caused the pressure to drop, leading to an increase in the gas saturation (as more gas comes out of solution) and a temperature drop that increases over time because of Joule-Thomson cooling. The minimum pressure is observed at the production well; the two additional wells have practically no impact (as expected) because of the very large volume of the elements in which they occur and their low production rates. As expected, the water and gas flows indicate fluid movement toward the central production well. Note that, because of the location of the two wells away from the center, flow toward these wells from both directions is also observed.

The additional output files **`WellZ_Time_Series,`** **`IntRR_Time_Series`** and **`Wells_Time_Series`** and (see input file **Test1** in the Appendix or on the memory stick) have the user-defined names specified in **Test1** and represent time series of data at a subdomain, through an interface and through a source/sink group, respectively. The data in each one of these files are clearly identified and their units are specified. In a continuation run (to be attempted during the training session), these files need to remain in the directory of the **T+RGB** execution because they provide vital information. The **T+RGB** code reads the last line of the data in each file, and uses some of these data in order to seamlessly continue the computation of the cumulative quantities of parameters of interest.

6.3. Problem Test2

This problem is a variation of that in **`Test1`**, from which it differs in the following aspects:

- Salt is now considered
- Klinkenberg effects are included
- Gas sorption is included
- Diffusion is included
- It has a single well at the center of the cylindrical reservoir

The reader is encouraged to (a) identify the data in the input file that enable these additional features, (b) run the **`Test2`** problem, and (c) compare the results to those from the run(s) in **`Test1`**. One of the important observations from the results of this simulation is the evolution of a solid phase because of the precipitation of salt as halite.

6.4. Problem Test3

This problem is another variation of that in **`Test1`**, from which it differs in the following aspects:

- Salt is now considered
- Klinkenberg effects are included
- The dry gas is composed of two gases (CH_4 and C_2H_6), and these are treated as a pseudo-component of invariable composition during the simulation
- Gas sorption is included
- The initial conditions are now single-phase (aqueous), with dissolved gas
- It has a single well at the center of the cylindrical reservoir

As before, the novice **T+RGB** user is encouraged to (a) identify the data in the input file that enable these additional features of this illustrative example, (b) run the **`Test3`** problem, and (c) compare the results to those from the run(s) in **`Test1`**. One of the important observations from the results of this simulation is the evolution of a gas phase because of gas exsolution and salting out.

6.5. Problems Test4 and Test5

This problem is another variation of that in **`Test1`**, from which it differs in the following aspects:

- Salt is now considered
- Klinkenberg effects are included
- The dry gas is composed of two gases (CH_4 and C_2H_6) in **`Test4`** and 4 gases in **`Test5`**, and these are treated as individual components, i.e., they are tracked independently
- Gas sorption is included
- The initial conditions are now single-phase (aqueous), with dissolved gas
- It has a single well at the center of the cylindrical reservoir

As before, the novice **T+RGB** user is encouraged to (a) identify the data in the input file that enable these additional features of this illustrative example, (b) run the **`Test4`** and **`Test5`** problems, (c) compare the results to those from the run(s) in **`Test1`**, and (d) run variations of these problems by modifying several inputs to determine the sensitivity of the results to these parameters and to the various computational options available in the code.

One of the important observations from the results of these two simulations is the evolution of a gas phase because of gas exsolution and salting out.

6.6. ProblemV1: Real gas transient flow in a cylindrical reservoir

Using the concept of pseudo-pressure, *Fraim and Wattenbarger* [1986] developed a solution to the problem of transient flow in a finite cylindrical real-gas reservoir with a producing vertical well at its center, described as:

$$p_D = \frac{1}{2} E_i \left(\frac{r_D^2}{4t_D} \right) \tag{6.1}$$

where E_i denotes the exponential integral,

$$p_D = \frac{kh}{q_V B \mu} \left(\psi_0 - \psi \right), \quad r_D = \frac{r}{r_w}, \quad t_D = \frac{k}{\phi \mu c_t r_w^2} t, \quad \psi = 2\int_{p_r}^{p} \frac{p}{\mu z} dp, \tag{6.2}$$

ψ is the pseudo-pressure, r is the radius, r_w is the well radius [m], p is the pressure [Pa], p_r is a reference pressure [Pa], c_t is the total compressibility [Pa^{-1}], q_V is the volumetric production rate [ST m^3/s], B is the formation volume factor, and h is the reservoir thickness. The subscript *0* indicates initial conditions, and the subscript *D* denotes dimensionless variables.

The data used in the simulation of this validation problem appear in **Table 6.1.** The input files are provided in the directory `Test_Problems_TRBG_V1.0` in the USB memory stick accompanying this manual. The gas was 100% CH_4. The cylindrical domain discretization involved a single layer, and a total of 32 logarithmically increasing Δr's. **Figure 6.1** shows a very good agreement of the analytical and the **T+RGB** numerical solutions at various sampling times. The **T+RGB** code yields an identical solution. Note that the problem was solved both isothermally and non-isothermally, and the difference between the two solutions was very small and localized in the vicinity of the well. This difference is attributed to Joule-Thomson cooling effects because of the bigger pressure drops and the high gas velocity at this location.

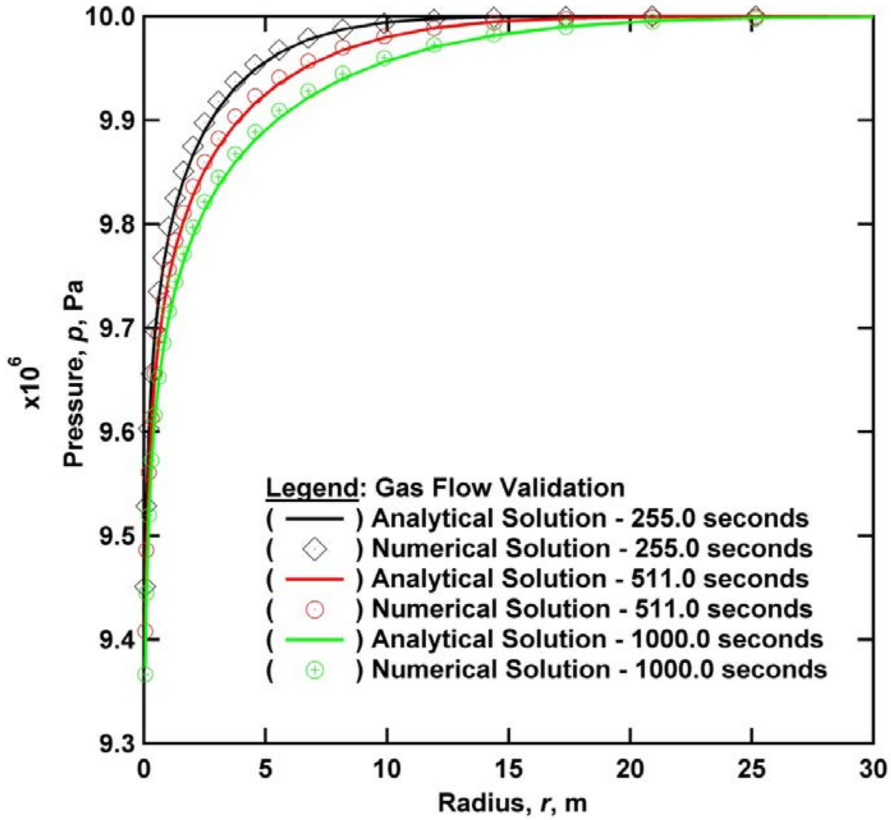

Figure 6.1. Validation of the T+RGB code against the analytical solution of *Fraim and Wattenbarger* [1987] in the ProblemV1 study of real gas transient flow in a cylindrical reservoir [*Moridis and Freeman*, 2014].

Table 6.1. Properties and conditions in Problem V1

Data Type	Values
Matrix permeability *k*	$3.04\text{x}10^{-14}$ m^2 (30.4 mD)
Reservoir thickness *h*	10 m
Well radius r_w	0.059 m
Reservoir radius r_e	100 m
Reservoir pressure *p*	10 MPa
Reservoir temperature *T*	60 ^{o}C
Reservoir porosity ϕ	0.30
Rock compressibility	$2\text{x}10^{-10}$ 1/Pa
Gas composition	100% CH_4
Gas EOS	Peng-Robinson

6.7. ProblemV2: Non-Darcy (Klinkenberg) Gas Flow

The *Klinkenberg* [1941] correction was originally developed to correct for the effect of gas slippage phenomena on permeability measurements of tight core samples. Depending on the flow rate, unconventional shale gas and tight gas sands may exhibit slip flow, or "Klinkenberg flow," in the reservoir itself. In order to correctly capture flow through such very low permeability media, the flow equations are derived in such a way that permeability is treated as a function of pressure that deviates from the theoretical permeability at infinite gas pressure according to $k = k_0(1+b/P)$.

As discussed earlier, there are several options for the computation of the Klinkenberg parameter *b* in **T+RGB,** see Section 4. *Wu et al.* [1988] used the pressure function $P_k = P + b$ to derived the following analytical solution to the problem of gas flow through an infinite cylindrical reservoir produced at a constant rate *q*:

The input parameters used in this problem are listed in **Table 6.2**. The input files are provided in the directory `Test_Problems_TRBG_V1.0` in the USB memory stick accompanying this manual. The gas was 100% CH_4. The cylindrical mesh used in the

T+RGB simulations involved a single layer and comprised 31 elements with logarithmically distributed *Δr* sizes. The agreement between the *Wu at al.* [1988] and the **T+RGB** solutions is excellent, as **Figure 6.2** clearly indicates. Additionally, given the short duration of the simulated period, the differences between the numerical predictions for isothermal and non-isothermal flow were practically negligible.

Table 6.2. Parameters in ProblemV2 of Klinkenberg Flow

k_∞	b	P_i	μ	ϕ	h	q	c_t	z
m^2	1/Pa	Pa	Pa-s		m	m^3/s	1/Pa	
3.0E-14	73830.6	1.00E7	1.44E-5	0.3	10	1.54E-2	1.07E-7	0.89

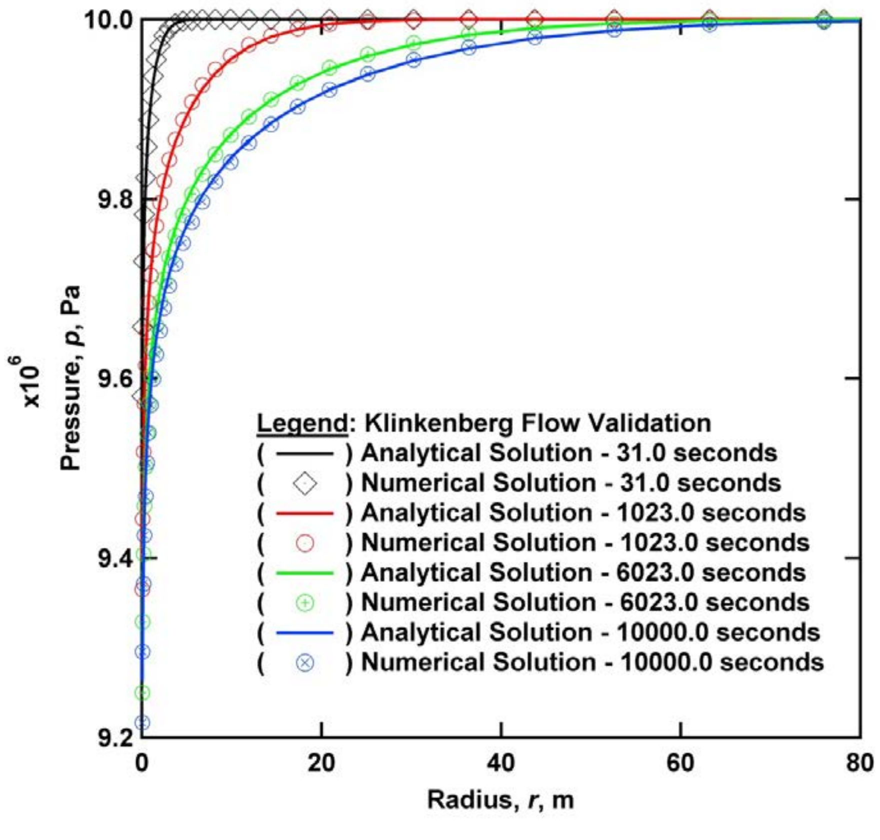

Figure 6.2. Validation of the T+RGB code against the analytical solution of *Wu et al.* [1988] in the ProblemV2 study of Klinkenberg flow in a cylindrical gas reservoir [*Moridis and Freeman*, 2014]**.**

6.8. ProblemV3: Flow Into a Vertical Fracture With a Well at its Center

The solution of *Cinco-Ley and Meng* [1988] describes flow from a rectangular reservoir into a finite-conductivity vertical fracture intersected by a well at its center. The single bi-wing vertical fracture is a stimulation treatment typically applied to vertical wells in low-permeability reservoirs. This complicated model transitions between two flow regimes over time. Bi-linear flow, where the dominant flow is through and perpendicular to the fracture face, is assumed at early times. At later times, the regime transitions into pseudo-radial flow.

The *Cinco-Ley and Meng* [1988] solution assumes flow for a slightly compressible liquid. In our computations, we used water as the reservoir fluid. The input files are provided in the directory `Test_Problems_TRBG_V1.0` in the USB memory stick accompanying this manual. The properties and conditions used in the computations of two cases (differing only in the fracture permeability) in this problem are listed in **Table 6.3**. The Cartesian domain in the T+GW study involved a single layer, and was discretized into 60x60x1 = 3400 elements in (x,y,z). The comparisons in **Figure 6.3** between the analytical and the **T+RGB** solutions in the two cases (involving different values of $F_{CD} = k_f\, b_f/(k_m\, x_f)$, as k_f was different) show a very good agreement.

Table 6.3. Properties and Conditions in ProblemV3

Case	p_i	k_m	k_f	h	q	B	μ	ϕ_m	c_t	x_f	F_{cD}	b_f
	kPa	mm^2	mm^2	m	m^3/d		Pa.s		1/Pa	m		m
1	1.0E5	3.3E-3	3.0E3	10	172.8	1	4.91E-4	0.3	3.37E-10	20	10^3	0.022
2	1.0E5	3.3E-4	3.0E3	10	172.8	1	4.91E-4	0.3	3.37E-10	20	10^4	0.022

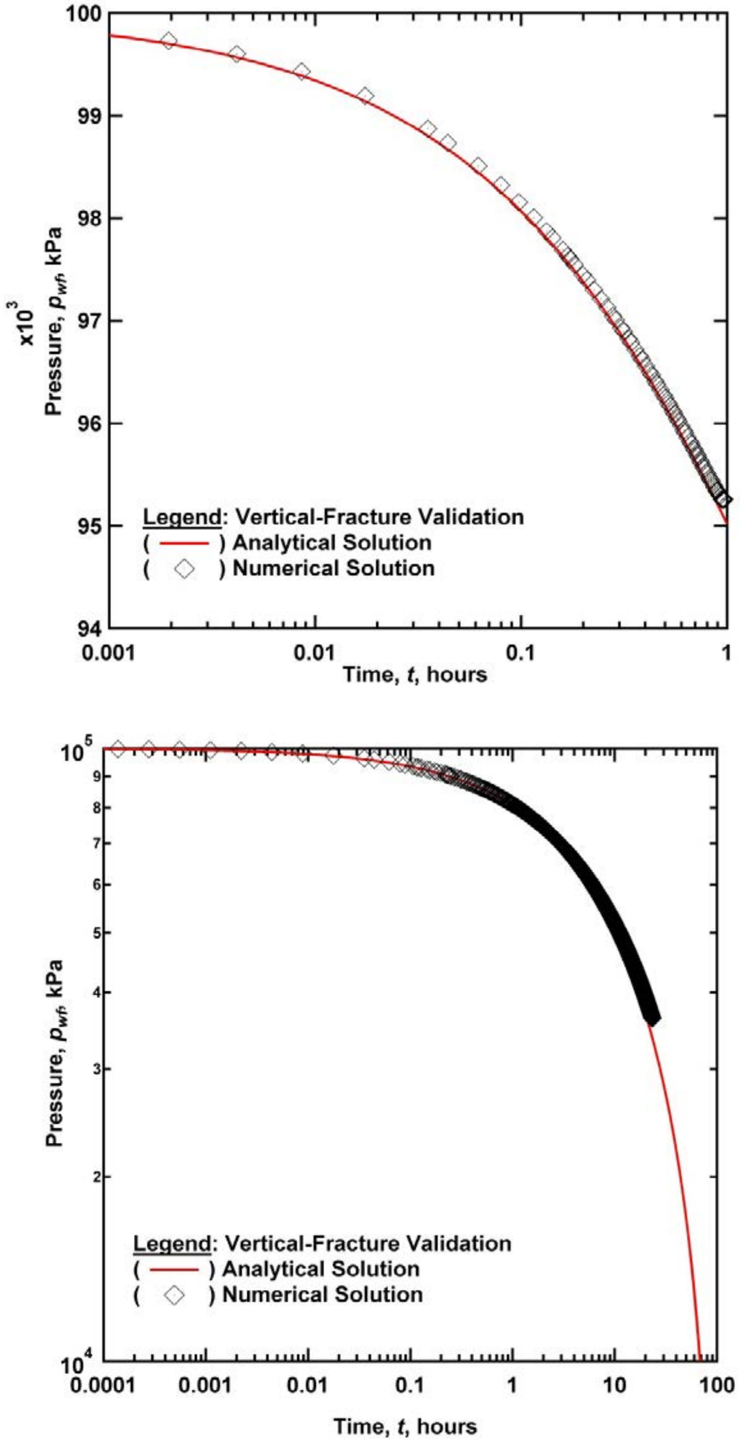

Figure 6.3. Validation of the T+RGB code against the analytical solutions of *Cinco-Ley and Meng* [1988] in the ProblemV3 study of flow into a vertical fracture intersected by a vertical well at its center. Case 1 (upper): $F_{CD} = 10$; Case 2 (lower): $F_{CD} = 10^4$ [*Moridis and Freeman*, 2014].

6.9. ProblemA1: Gas Production From a Multi-Fractured Shale Gas Reservoir Using a Horizontal Well

This **T+RGB** study focuses on a Cartesian 3D stencil of a horizontal well section that is typical of a Type I shale gas system (**Figure 6.4**), as defined and investigated by *Freeman* [2010] and *Moridis et al.* [2010]. Such systems involve the (usually hydraulically) induced primary fractures (PF), the undisturbed matrix, and the stress release fractures around the well. The data used in this simulation were as in *Freeman* [2010]. The surface area of the Cartesian system at the well was corrected to reflect its cylindrical geometry. The simulated 3D domain (**Figure 6.4**) represents the stencil of the horizontal well system, i.e., the smallest repeatable subdomain that can accurately describe the system behavior. Studies by *Olorode* [2011] and *Olorode et al.* [2013] have confirmed that such stencils are accurate representatives of the behavior of the entire system for very long production periods.

The discretization of the 3D domain involved subdivisions as small as mm-scale near the fracture face, and resulted in about 800,000 gridblocks. To develop the mesh file, we used an expanded version of the MESHMAKER facility available to the TOUGH+ code [*Moridis*, 2014] and its MINC option [*Pruess*, 1983], in addition to a short FORTRAN code written for this purpose. Two different media were considered: the matrix and the hydraulically induced fracture, which was represented by appropriate flow and thermal properties. The problem was solved both isothermally and non-isothermally. The gas was 100% CH_4, and its sorption onto the shale followed an equilibrium Langmuir isotherm.

Using the **T+RGB** code and assuming isothermal conditions, the predicted production rate when the well is operated at a constant bottomhole pressure P_w is shown in **Figure 6.5**, which also lists the data used in the simulation. Here we employ the the dimensionless variables commonly used in such studies, which are defined as:

$$t_D = \frac{k}{\varphi\mu c_t x_f^2}\frac{1}{[1+V_L]}\,t,\ \ q_D = \frac{B\mu}{kh(p_i - p_{wf})}\,q, \tag{6.4}$$

$$q_{Di}(t) = \frac{1}{t}\int_0^t q_D(\tau)\,d\tau,\ \ \text{and}\ \ q_{Did}(t) = -t\frac{dq_{Di}}{dt} \tag{6.5}$$

Figure 6.6 shows the distribution of the normalized pressure in the vicinity of the fracture face on the (x,y) plane along the length of the fracture at a height of 4 m above the well plane. Note the steep pressure gradients perpendicular to the fracture face that are the result of the very low permeability of the shale.

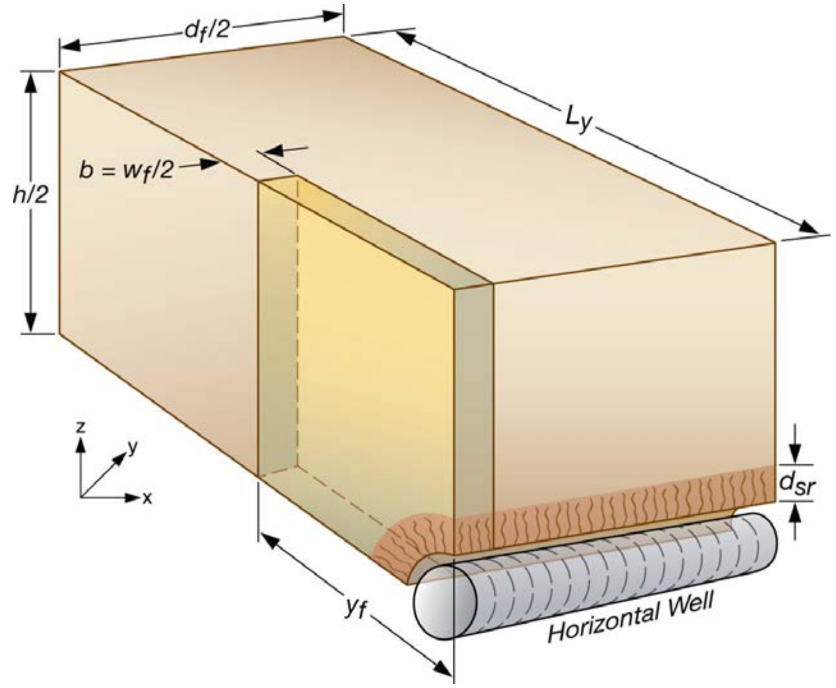

Figure 6.4. Stencil of a Type I system involving a horizontal well in a tight- or shale-gas reservoir [*Moridis et al.,* 2010].

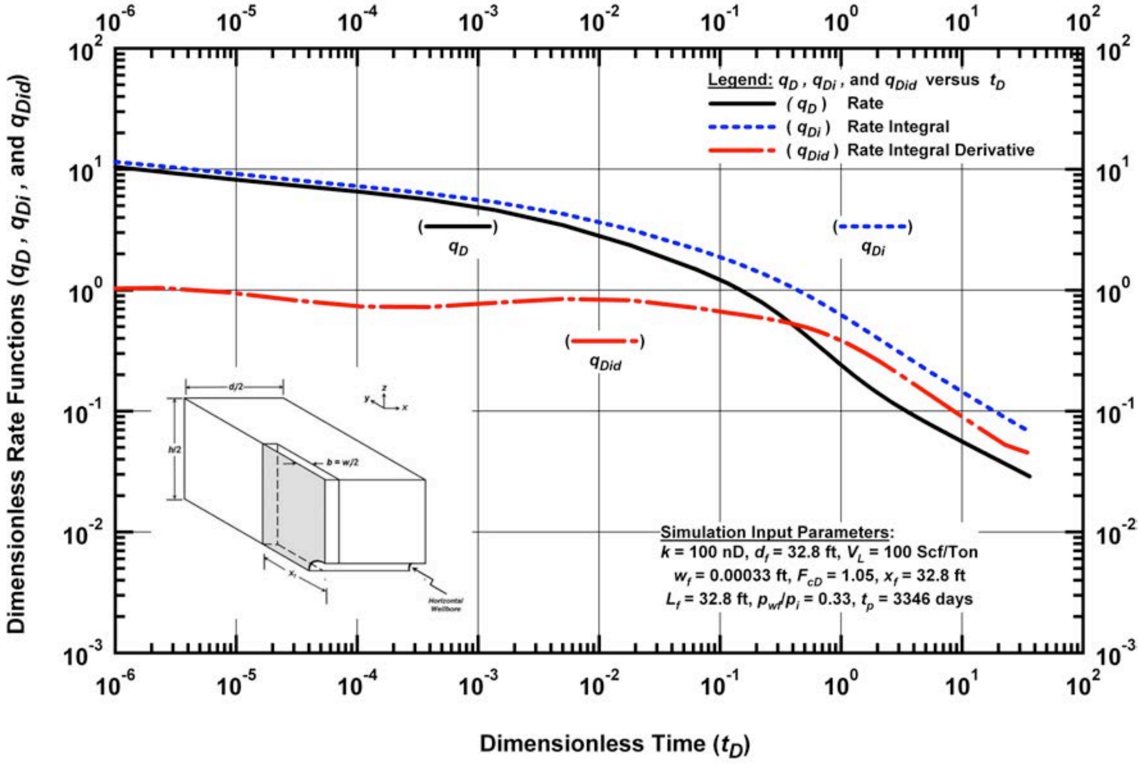

Figure 6.5. Prediction of gas production in the ProblemA1 study [*Freeman et al.*, 2010].

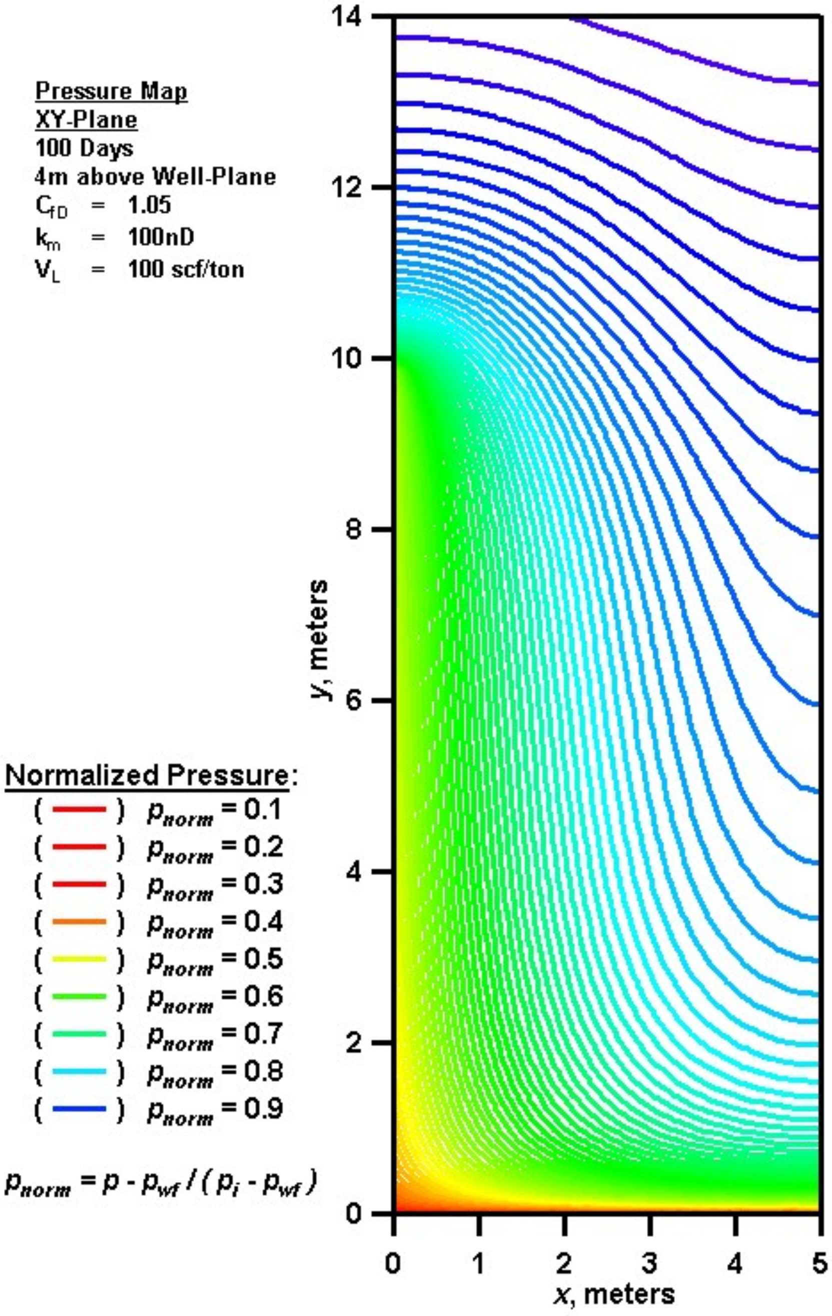

Figure 6.6. Pressure distribution in the vicinity of the hydraulically induced fracture in the shale gas system of ProblemA1 [*Freeman*, 2010]. Note the steep pressure gradient in the vicinity of the hydraulic fracture and of the horizontal well caused by the very low permeability of the shale.

PAGE LEFT INTENTIONALLY BLANK

7.0 Acknowledgements

The research described in this report has been funded by the U.S. Environmental Protection Agency through Interagency Agreement (DW-89-92235901-C) to the Lawrence Berkeley National Laboratory (a U.S. Department of Energy National Laboratory managed by the University of California under Contract No. DE-AC02-05CH11231), and by the Research Partnership to Secure Energy for America (RPSEA - Contract No. 08122-45) through the Ultra-Deepwater and Unconventional Natural Gas and Other Petroleum Resources Research and Development Program as authorized by the US Energy Policy Act (EPAct) of 2005. The authors express their thanks and appreciation to Dr. Alfredo Battistelli of SAIPEM SpA (Italy) for his valuable help on several issues regarding the constitutive relationships used in the code. The views expressed in this article are those of the authors and do not necessarily reflect the views or policies of the EPA.

PAGE LEFT INTENTIONALLY BLANK

8.0 References

Americal Petroleum Institute (API). Policy Issues: Facts about Shale Gas 2013. http://www.api.org/policy-and-issues/policy-items/exploration/facts_about_shale_gas

Andersen, G., A. Probst, L. Murray and S. Butler, An accurate PVT model for geothermal fluids as represented by H_2O-CO_2-NaCl mixtures. Proceedings, Seventeenth Workshop on Geothermal Reservoir Engineering, **17**, 239-248, Stanford University, Stanford, California, January 29-31, 1992.

Anderson, D.M., M. Nobakht and S. Moghadam, Analysis of Production Data from Fractured Shale Gas Wells. Paper SPE 131787, 2010 SPE Unconventional Gas Conference, Pittsburgh, Pennsylvania, USA. doi: 10.2118/131787-MS

Barree R.D., and M.W. Conway, Multiphase non-Darcy flow in proppant packs, Paper SPE 109561, 2007 Annual Technical Conference and Exhibition, Anaheim, CA, 11–14 Nov 2007.

Battistelli, A., Improving the Treatment of Saline Brines in EWASG for the Simulation of Hydrothermal Systems, Proceedings, TOUGH Symposium 2012, Berkeley, California, September 17-19, 2012.

Bello, R.O. and R.A. Wattenbarger, Rate Transient Analysis in Naturally Fractured Shale Gas Reservoirs. Paper SPE 114591, CIPC/SPE Gas Technology Symposium 2008 Joint Conference, Calgary, Alberta, Canada. doi: 10.2118/114591-MS

Bird, R.B., W.E. Stewart, and E.N. Lightfoot, *Transport Phenomena*. New York: John Wiley & Sons, Inc., 2007.

Blasingame, T.A. and B.D. Poe Jr., Semianalytic Solutions for a Well with a Single Finite-Conductivity Vertical Fracture. Paper SPE 26424, 1993 SPE Annual Technical Conference and Exhibition, Houston, Texas, USA. doi: 10.2118/26424-MS.

Chou, I.M., Phase Relations in the System NaCl–KCl–H2O: III: Solubilities of Halite in Vapor-Saturated Liquids Above 445 °C and Redetermination of Phase Equilibrium Properties in the System NaCl–H2O, *Geochim. Cosmochim. Acta*, 51, 1965–1975, 1987

Chung, T.H., M. Ajlan, L.L. Lee and K.E. Starling, Generalized multiparameter correlation for nonpolar and polar fluid transport properties, *Ind. Eng. Chem. Res*., **27**(4), 671-679, 1988 (doi: 10.1021/ie00076a024)

Cinco-Ley, H. and H.-Z. Meng, Pressure Transient Analysis of Wells With Finite Conductivity Vertical Fractures in Double Porosity Reservoirs. Paper SPE 18172-MS presented at the SPE Annual Technical Conference and Exhibition, Houston, Texas, 2-5 October 1988. http://dx.doi.org/10.2118/18172-MS.

Cinco-Ley, H., F. Samaniego, and N. Dominguez, Transient pressure behavior for a well with a finite-conductivity vertical fracture, *SPE Journal* **18**(4): 253-264, 1978. SPE 6014-PA. http://dx.doi.org/10.2118/6014-PA

Cipolla, C.L., E. Lolon, J. Erdle et al., Modeling Well Performance in Shale-Gas Reservoirs. Paper SPE 125532, 2009 SPE/EAGE Reservoir Characterization and Simulation Conference, Abu Dhabi, UAE. doi: 10.2118/125532-MS

Civan, F., Effective Correlation of Apparent Gas Permeability in Tight Porous Media. *Transp. in Porous Med.*, 83, 375-384, 2008 (doi: 10.1007/s11242-009-9432-z)

Clarkson, C.R. and R.M. Bustin, Binary Gas Adsorption/Desorption Isotherms: Effect of Moisture and Coal Composition Upon Carbon Dioxide Delectivity Over Methane. *International Journal of Coal Geology*, **42**, 241-271, 1999.

Coles, M. E., and K. J. Hartman, Non-Darcy Measurements in Dry Core and the Effect of Immobile Liquid, Paper SPE 39977, 1998 SPE Gas Technology Symposium, Calgary, Canada, March 15–18, 1998.

Driesner, T., The System H_2O-NaCl. II. Correlation Formulae for Phase Relations in Temperature-Pressure-Composition Space from 0 to 1000°C, 0 to 5000 bar, and 0 to 1 X_{NaCl}, *Geochimica et Cosmochimica Acta* **71**, 4880-4901, 2007.

Driesner, T. and C.A. Heinrich, The System H_2O-NaCl. I. Correlations for molar volume, enthalpy, and isobaric heat capacity from 0 to 1000 degrees C, 1 to 5000 bar, and 0 to 1 X-NaCl, *Geochimica et Cosmochimica Acta* **71**, 4902-4919, 2007.

Cooper, J. W., X. Wang, and K.K. Mohanty, Non-Darcy-Flow Studies in Anisotropic Porous Media, *SPEJ*, 334–341, 1999.

Ergun, S., Fluid Flow Through Packed Column, *Chemical Engineering Progress,* **48**(2), 89–94, 1952.

Computer Modeling Group (CMG). 2013 GEM General Release (GEM 2013.10), http://www.cmgl.ca/software/soft-gem

Doronin, G.G. and N.A. Larkin. On dusty gas model governed by the Kuramoto-Sivashinsky equation. *Computational and Applied Mathematics,* **23**(1), 67-80, 2004.

Doughty, C., Investigation of conceptual and numerical approaches for evaluating moisture, gas, chemical, and heat transport in fractured unsaturated rock, *J. Contam.t Hydrol.*, **38**(1-3), 69-106, 1999

Finsterle, S., Implementation of the Forchheimer Equation in iTOUGH2, Project Report, Lawrence Berkeley National Laboratory, Berkeley, Calif., 2001.

Florence, F.A., J.A. Rushing, K.E. Newsham and T.A. Blasingame, Improved permeability prediction relations for low-permeability sands, SPE paper 107954, SPE Rocky Mountain Oil and Gas Technology Symposium, 16–18 April, Denver, Colorado, 2007.

Freeman, C.M., Study of flow regimes in multiply-fractured horizontal wells in tight gas and shale gas reservoir systems, M.Sc. Thesis, Petroleum Engineering Department, Texas A&M University, 2010.

Freeman, C.M., G.J. Moridis, and T.A. Blasingame. A Numerical Study of Microscale Flow Behavior in Tight Gas and Shale Gas Reservoir Systems. *Transp. in Porous Med., 90*(1): 253-268, 2011 (doi: 10.1007/ s11242-011-9761-6)

Fraim, M.L., and R.A. Wattenbarger. Gas Reservoir Decline Curve Analysis Using Type Curves with Real Gas Pseudopressure and Pseudotime, *SPEFE*, 671-682, 1987.

Frederick, D.C., and R. M. Graves, New Correlation to Predict Non-Darcy Flow Coefficients at Immobile and Mobile Water Saturation, Paper SPE 28451, Proceedings of the 1994 SPE Annual Technical Conference and Exhibition, 915–921, New Orleans, LA, Sept. 25–28, 1994.

Freeman, C.M., G.J. Moridis, D. Ilk, and T.A. Blasingame, A Numerical Study of Performance for Tight Gas and Shale Gas Reservoir Systems, *Journal of Petroleum Science and Engineering*, **108**, 22-39, 2013 (http://dx.doi.org/10.1016/j.petrol. 2013.05.007).

Forchheimer, P., Wasserbewewegung durch Boden, *ZVDI* 45, 1781, 1901.

Gao, C., J.W. Lee, J.P. Spivey, and M.E. Semmelbeck. Modeling multilayer gas reservoirs including sorption effects, SPE paper 29173, SPE Eastern Regional Conference & Exhibition, Charleston, West Virginia, 8-10 November, 1994.

Geertsma, J., Estimating the Coefficient of Inertial Resistance in Fluid Flow Through Porous Media, *SPEJ*, 445–450, 1974.

Gringarten, A.C., Unsteady-State Pressure Distributions Created by a Well with a Single Horizontal Fracture, Partial Penetration, or Restricted Entry. Ph.D. Dissertation, Stanford University, Stanford, California, USA, 1971.

Gringarten, A.C., H.J. Ramey, J., and R. Raghavan, Unsteady-State Pressure Distributions Created by a Well with a Single Infinite-Conductivity Vertical Fracture. *SPE Journal* **14** (4), 1974. doi: 10.2118/4051-PA.

Haas, J.L. Jr., Physical Properties of the Coexisting Phases and Thermochemical Properties of the H2O Component in Boiling NaCl Solutions, USGS Bulletin 1421-A, Washington, DC, 73 pp., 1976.

Houze, O., E. Tauzin, V. Artus et al., The Analysis of Dynamic Data in Shale Gas Reservoirs - Part 1. Company report, Kappa Engineering, Houston, Texas, USA, 2010.

Janicek, J. D., and D. L. Katz, Applications in Unsteady State Gas Flow Calculations, *Proc.*, Univ. of Michigan Research Conference, June 20, 1955.

Jayakumar, R., V. Sahai and A. Boulis, A Better Understanding of Finite Element Simulation for Shale Gas Reservoirs through a Series of Different Case Histories. Paper SPE 142464, 2011 SPE Middle East Unconventional Gas Conference and Exhibition, Muscat, Oman. doi: 10.2118/142464-MS

Jones, S. C., A rapid accurate unsteady-state Klinkenberg parameter, *SPE Journal* 383–397, 1972.

Jones, F.O. and W.W. Owen, A laboratory study of low permeability gas sands, *J. Pet. Technol.*, **32**, 1631-1640, 1980.

Katz, D. L. et al., *Handbook of Natural Gas Engineering*. McGraw-Hill, New York, 1959.

Kim, J., and G.J. Moridis, Development of the T+M coupled flow-geomechanical simulator to describe fracture propagation and coupled flow-thermal-geomechanical processes in tight/shale gas systems, *Computers & Geosciences, 60*, 184-198, 2013 (doi: 10.1016/j.cageo.2013.04.023)**.**

Lee B.I. and M.G. Kesler, A Generalized Thermodynamic Correlation Based on Three-

Parameter Corresponding States, *AIChE J.*, **21**(3), 510-527, 1975.

Liu, X., F. Civan, and R. D. Evans, Correlation of the Non-Darcy Flow Goefficient, *JCPT*, **34**(10), 50–54, 1995.

Lorenz, S., D. Maric and C. Rirschl, Eine Analytische Funktion Zur Bestimmung der Enthalpie Waesseriger NACL-Loesungen, Report ISTEC-A-447, Institut Fuer Sicherheitstechnologie, Koeln, Germany, March 2000.

Mason, E.A. and A.P. Malinauskas, Gas Transport in Porous Media: The Dusty Gas Model. Elsevier, New York, 1983.

Mao, S. and Z. Duan, The viscosity of Aqueous Alkali-Chloride Solutions up to 623 K, 1000 bar and High Ionic Strength, *International Journal of Thermophysics*, 30, 1510-1523, 2009.

Mattar, L., Production Analysis and Forecasting of Shale Gas Reservoirs: Case History-Based Approach. Paper SPE 119897, 2008 SPE Shale Gas Production Conference, Fort Worth, Texas, USA. doi: 10.2118/119897-MS

Medeiros, F., E. Ozkan, E., and H. Kazemi, A Semianalytical, Pressure-Transient Model for Horizontal and Multilateral Wells in Composite, Layered, and Compartmentalized Reservoirs. Paper SPE 102834, 2006 SPE Annual Technical Conference and Exhibition, San Antonio, Texas, USA. doi: 10.2118/102834-MS.

Michaelides, E.E., Thermodynamic properties of geothermal fluids, *Geotherm. Resour. Counc. Trans*., Vol. 5, 361-364; (United States) 5.CONF-811015, 1981.

Miller, A.B., A Brine-Steam Properties Computer Program for Geothermal Energy Calculations, LLNL Report UCRL-52495, Livermore, CA, June 1978.

Miller, M.A., C.D. Jenkins, and R.R. Rai, Applying Innovative Production Modeling Techniques to Quantify Fracture Characteristics, Reservoir Properties, and Well Performance in Shale Gas Reservoirs. Paper SPE 139097, 2010 SPE Eastern Regional Meeting, Morgantown, West Virginia, USA. doi: 10.2118/139097-MS.

Moridis, G.J. and K. Pruess, User's Manual of the TOUGH+ v1.5 Core Code: A General Purpose Simulator of Non-Isothermal Flow and Transport Through Porous and Fractured Media, Lawrence Berkeley National Laboratory Report LBNL-6869E, August 2014.

Moridis, G.J., T.A. Blasingame, and C.M. Freeman, Analysis of Mechanisms of Flow in Fractured Tight-Gas and Shale-Gas Reservoirs, Paper SPE 139250, SPE Latin American & Caribbean Petroleum Engineering Conference, Lima, Peru, 1–3 December 2010.

Olorode, O., Numerical Modeling and Analysis of Shale-Gas Reservoir Performance Using Unstructured Grids, M.Sc. Thesis, Petroleum Engineering Department, Texas A&M University, 2011.

Olorode, O.M., Freeman, C.M., G.J. Moridis, and T.A. Blasingame, High-Resolution Numerical Modeling of Complex and Irregular Fracture Patterns in Shale Gas and Tight Gas Reservoirs, *SPE Reservoir Evaluation & Engineering,* **16**(4), 443-455, 2013 (http://dx.doi.org/10.2118/152482-PA)**.**

Pan, Z. and L.D. Connell, Comparison of adsorption models in reservoir simulation of enhanced coalbed methane recovery and CO2 sequestration in coal. Int. J. Greenhouse Gas Control, **3**(1), 77–89, 2009. http://dx.doi.org/10.1016/j.ijggc. 2008.05.004.

Peng, D.Y., and D.B. Robinson. A New Two-Constant Equation of State, *Indust. and Engr. Chemistry: Fundamentals* **15**, 59-64, 1976.

Phillips, S.L., A. Igbene, J.A. Fair, H. Ozbek and M. Tavana, A Technical Databook for Geothermal Energy Utilization, Lawrence Berkeley National Laboratory Report LBL-12810, Berkeley, CA, 46 pp., 1981.

Pruess, K., GMINC - A Mesh Generator for Flow Simulations in Fractured Reservoirs, Lawrence Berkeley Laboratory Report LBL-15227, Berkeley, CA, March 1983.

Pruess, K., C. Oldenburg, and G. Moridis. TOUGH2 User's Guide, Version 2.0, Report LBNL-43134, Lawrence Berkeley National Laboratory, Berkeley, Calif., 1999.

Pruess, K., C. Oldenburg, and G. Moridis. TOUGH2 User's Guide, Version 2.1, Report LBNL-43134, Lawrence Berkeley National Laboratory, Berkeley, Calif., 2012.

Quiñones-Cisneros S.E., C.K. Zéberg-Mikkelsen and E.H. Stenby, The Friction Theory (f-theory) for Viscosity Modeling, *Fluid Phase Equilib.,* **169**, 249–276, 2000.

Redlich, O. and J.N.S. Kwong, On The Thermodynamics of Solutions, *Chem. Rev.* **44** (1): 233–244, 1949.

Sampath, K. and C.W. Keighin, Factors Affecting Gas Slippage in Tight Sandstones, SPE Paper 9872, Proceedings of the SPE/DOE Symposium on Low Permeability Reservoirs, Denver, Colorado, May 27-29, 409-416, 1981.

Schettler, P.D., and C.R. Parmely, Contributions to total storage capacity in devonian shales, SPE paper 23422, SPE Eastern Regional Meeting, Lexington, Kentucky, 22-25 October, 1991.

Silvester, L.F. and K.S. Pitzer, Thermodynamics of Electrolytes, X. Enthalpy and the Effects of Temperature on the Activity Coefficients, *Journal of Solution Chemistry*, 7, 327-337, 1978.

Soave, G., Equilibrium constants from a modified Redlich–Kwong equation of state, *Chemical Engineering Science* **27** (6): 1197–1203, 1972.

Sourirayan, S. and G.C. Kennedy, The System H2O-NaCl at Elevated Temperatures and Pressures, *American Journal of Science*, 260, 115-141, 1962.

Sclumberger (SLB) Software, 2013 ECLIPSE for Unconventionals, http://www. software.slb.com/products/foundation/pages/eclipse-unconventionals.aspx

TecPlot, Inc., *Tecplot 10 User's Manual*, Bellevue, Washington, 2003.

Thauvin, F., and K.K. Mohanty, Network Modeling of Non-Darcy Flow Through Porous Media, *Transp. Porous Media*, **31**, 19–37, 1998.

U.S. Energy Information Administration (EIA), 2008; 2011; 2012. Annual Energy Review. /http://www.eia.gov/totalenergy/data/annual/

Warlick, D.N., Gas Shale and CBM Development in North America. Oil and Gas Journal. **3**(11), 1-8, 2006. http://www.ogfj.com/index/article-tools-template/printArticle /articles/oil-gas-financial-journal/ volume-3/issue-11/features/ gas-shale-and-cbm-development-in-north-america.html.

Warren, J.E. and P.J. Root. The Behavior of Naturally Fractured Reservoirs, *SPEJ* 245-55; *Trans*. AIME, **228,** 1963.

Wattenbarger, R.A. and H.J. Ramey, Gas well testing with turbulence, damage and wellbore storage, SPE 1835, *J. Pet. Tech.*, 877-884, 1968.

Webb, S.W., Gas-Phase Diffusion in Porous Media - Evaluation of an Advective-Dispersive Formulation and the Dusty Gas Model for Binary Mixtures, *J. Por. Media,* Vol. 1, No. 2, pp. 187 - 199, 1998.

Webb, S.W. and K. Pruess, The Use of Fick's Law for Modeling Trace Gas Diffusion in Porous Media. *Transp. Porous Media,* **51***,* 327-341, 2003.

Wu, Y., Pruess, K., and P. Persoff. Gas Flow in Porous Media with Klinkenberg Effects. *Transp. Porous Media*, **32**, 117-137, 1988.

Wu, Y.S., B. Lai, J.L. Miskimins, P. Fakcharoenphol and Y. Di, Analysis of Multiphase Non-Darcy Flow in Porous Media, Transport in Porous Media, **88**, 205–223, 2011 (doi: 10.1007/s11242-011-9735-8).

D.Yang, J. M., Thermophysical properties, in: Physical Properties Data for Rock Salt, edited by L. H. Gevantman, Monograph 167, 205-221, National Bureau of Standards, Washington, 1981.

PAGE LEFT INTENTIONALLY BLANK

APPENDIX

A Sample Input File

PAGE LEFT INTENTIONALLY BLANK